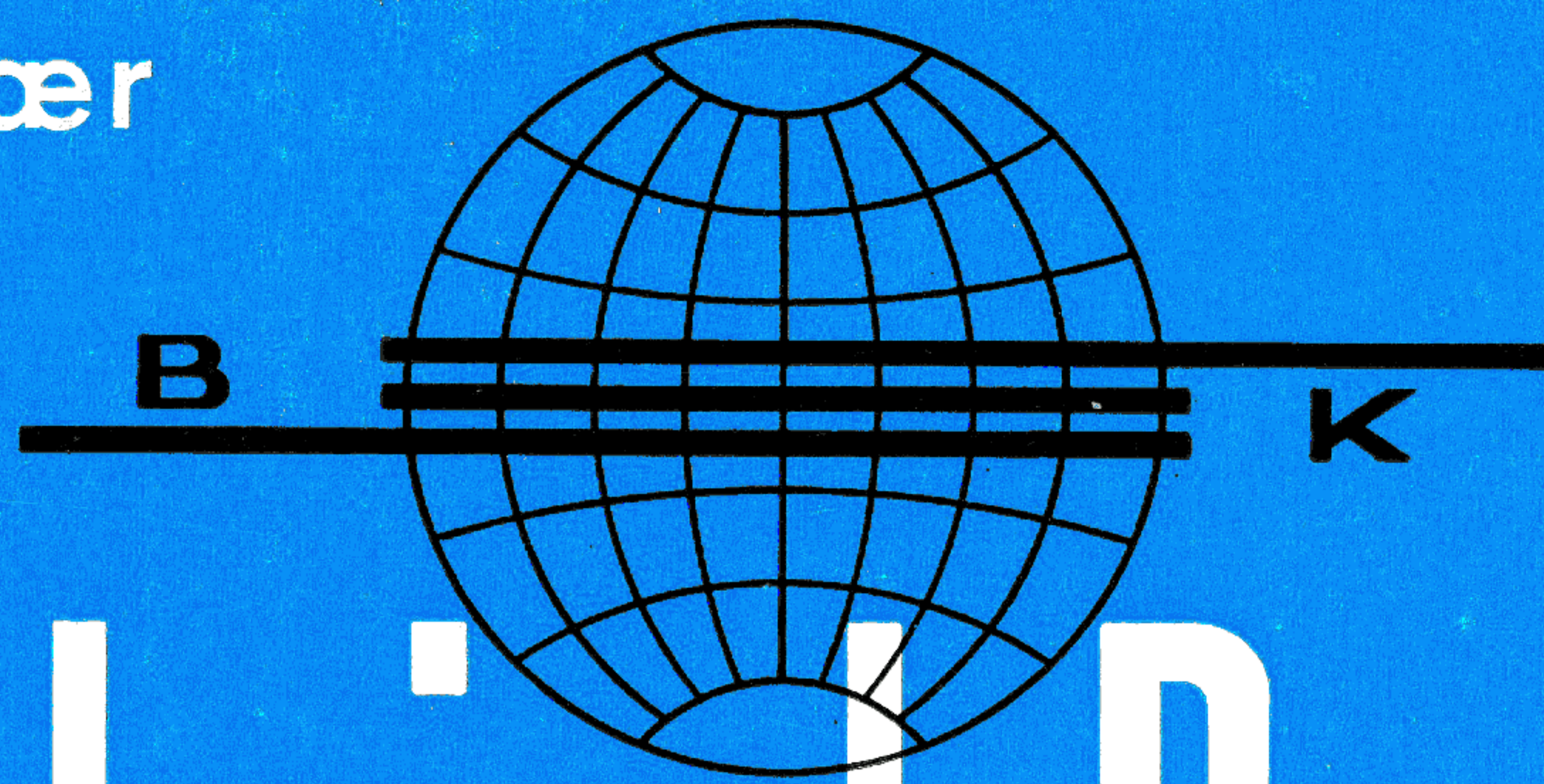


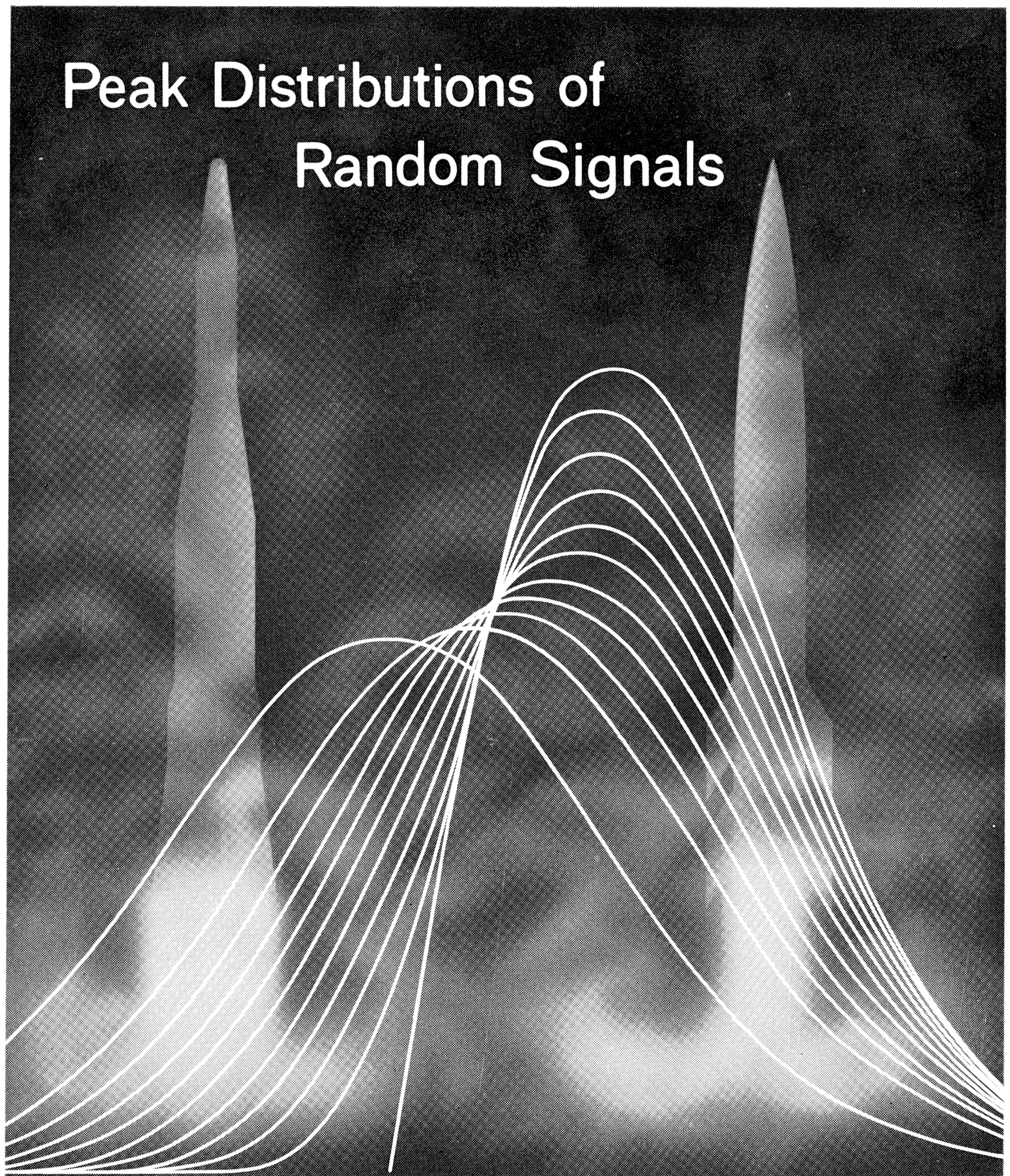
Brüel & Kjær



# Technical Review

To Advance Techniques in Acoustical, Electrical, and Mechanical Measurement

Peak Distributions of  
Random Signals



**PREVIOUSLY ISSUED NUMBERS OF  
BRÜEL & KJÆR TECHNICAL REVIEW**

- 1-1958 Measurement of the Complex Modulus of Elasticity.  
2-1958 Vibration Testing of Components.  
Automatic Level Regulation of Vibration Exciters.  
3-1958 Design Features in Microphone Amplifier Type 2603  
and A. F. Spectrometer Type 2110.  
A true RMS Instrument.  
4-1958 Microphonics in Vacuum Tubes.  
1-1959 A New Condenser Microphone.  
Free Field Response of Condenser Microphones.  
2-1959 Free Field Response of Condenser Microphones (Part II)  
3-1959 Frequency-Amplitude Analyses of Dynamic Strain and  
its Use in Modern Measuring Technique.  
4-1959 Automatic Recording of Amplitude Density Curves.  
1-1960 Pressure Equalization of Condenser Microphones  
and Performance at Varying Altitudes.  
2-1960 Aerodynamically Induced Noise of Microphones and  
Windscreens.  
3-1960 Vibration Exciter Characteristics.  
4-1960 R.M.S. Recording of Narrow Band Noise with the Level  
Recorder Type 2305.  
1-1961 Effective Averaging Time of the Level Recorder  
Type 2305.  
2-1961 The Application and Generation of Audio Frequency  
Random Noise.  
3-1961 On the Standardisation of Surface Roughness.  
4-1961 Artificial Ears.  
1-1962 Artificial Ears part 2.  
2-1962\* Loudness Evaluation.  
3-1962\* Stereophonic Gliding Frequency Records.  
4-1962\* On the Use of Warble Tone and Random Noise for  
Acoustic Measurement Purposes.  
Problems in Feedback Control of Narrow Band Random  
Noise.  
1-1963\* Miniature Microphones. Checking of R.M.S. Instruments.  
2-1963\* Quality Control by Noise Analysis.  
A.F. Nonlinear Distortion Measurement by Wide Band  
Noise.

---

\* Also published in French.

# TECHNICAL REVIEW

No. 3 – 1963

# CONTENTS

	Page
<i>Effects of Spectrum Non-linearities upon the Peak Distribution of Random Signals</i> .....	5
<i>Appendix</i>	
Brief Theory of the Distribution of Maxima .....	30

## **ABSTRACT**

The importance of noise and vibration peaks and their damaging effects is briefly described. A study is made on the dependency of the peak distribution upon the shape of the vibration spectrum using some of the results obtained by S. O. Rice. It is shown that a modification of Rice's exact theory will furnish good approximations in practice, and that the approximations are simple to "handle" mathematically. Furthermore, it makes the determination of peak probability density curves a simple matter when the frequency response of the system is known (and independent of excitation level), and the excitation is known to be Gaussian random noise.

## **SOMMAIRE**

Après un bref rappel de l'importance des valeurs de crêtes en ce qui concerne les effets dangereux des bruits et vibrations, l'article présente une étude de l'inter-dépendance entre la répartition statistique des crêtes et le spectre correspondant, basée sur certains résultats des travaux de S. O. RICE. On montre qu'une modification de la théorie de Rice permet d'obtenir des approximations simples à traiter mathématiquement et utilisables en pratique. De plus, on peut alors facilement déterminer la répartition statistique des crêtes d'après la courbe de réponse du système considéré, pour tout niveau d'excitation gaussienne.

## **ZUSAMMENFASSUNG**

Scheitel von Geräuschen und mechanischen Schwingungen können eine zerstörende Wirkung haben. An Hand der Ergebnisse von S. O. Rice wird der Einfluß des Schwingungsspektrums auf die Scheitelverteilung untersucht. Durch Modifikation der exakten Theorie nach Rice erhält man eine praktisch brauchbare Annäherung, die mathematisch einfach zu behandeln ist. Die Methode erleichtert die Bestimmung der Scheitelhäufigkeitskurven, wenn der Frequenzgang des Systems bekannt und unabhängig vom Erregungspegel ist, und wenn ferner als Erregungssignal Gauß'sches Breitbandrauschen angenommen wird.

# Effects of Spectrum Non-linearities upon the Peak Distribution of Random Signals.

By

*Jens Trampe Broch, Dipl. Ing. E.T.H.*

## **Introduction.**

In the course of the past decades the analysis of random noise and vibration signals has gained increasing importance, due mainly to the development of fast travelling vehicles. However, in daily life too, the importance of random signals such as factory and traffic noise, has increased rapidly in the later years.

As regards audible noise, great efforts have been, and are being, made to develop complete theories for hearing damage and the "intrusiveness" of these sounds. In the field of vibration the study of the fatigue of metals and the sudden malfunction of equipment and parts, due to high vibration peaks, have been intimately related to the study of random signals.

Because of their nature random noise and vibration signals can be mathematically described only by means of statistical methods and a number of investigators have successfully applied these methods in their studies. In this paper the peak response of various electromechanical analogues to random inputs are being investigated, and extensive use has been made of some of the results obtained by S. O. Rice and described in his now "classic" work: "Mathematical Analysis of Random Noise".

Some special measuring arrangements have been developed to check the results experimentally, and the B & K Random Noise Generator Type 1402 was used as signal source during the experimental part of the work. The Type 1402 Noise Generator has been found especially well suited for this kind of investigation due to its symmetrical Gaussian instantaneous value distribution and the experimental curves have been measured up to around  $3.5 \sigma$  values. At higher amplitude values, the Type 1402 Noise Generator shows slight deviations from a truly Gaussian distribution, and the measuring time involved in investigations at the high  $\sigma$ -values, makes the use of these values unattractive. It is assumed that an experimental verification of the theoretical results up to the above mentioned values of  $3.5 \sigma$  will suffice.

## **Statement of the Problem.**

Rice has given a general formula for the distribution of peak values (noise signal maxima) as a function of spectrum shape. He also solved the equation for the case of an ideal low-pass filter with a "flat" passband, and gave the result for an ideal, "infinitely narrow" band-pass filter. The two results are shown in Fig. 1. One of the questions arising immediately from a study of Fig. 1 is: How will the distribution be affected by other types of random

signal frequency spectra? If the band-width of the band-pass filter is increased from “infinitely narrow” to a low-pass filter, one would expect the distribution curves to lie between those given in Fig. 1. It can be verified both theoretically and experimentally that this is the case. However, the slope of the spectrum also plays an important role and in some cases an exact mathematical treatment may lead to results which give only little relation to practical experience. The reason for this is that the mathematical theory does not distinguish between very small peaks and notches, which may be of little practical importance, and relatively great peaks and notches, which may be of considerable importance with regard to the malfunction of essential equipment. In the following, an approximate theory which covers a wide range of commonly encountered frequency spectra will be proposed, and it is shown how the distribution of important peaks depends upon the shape of the spectrum.

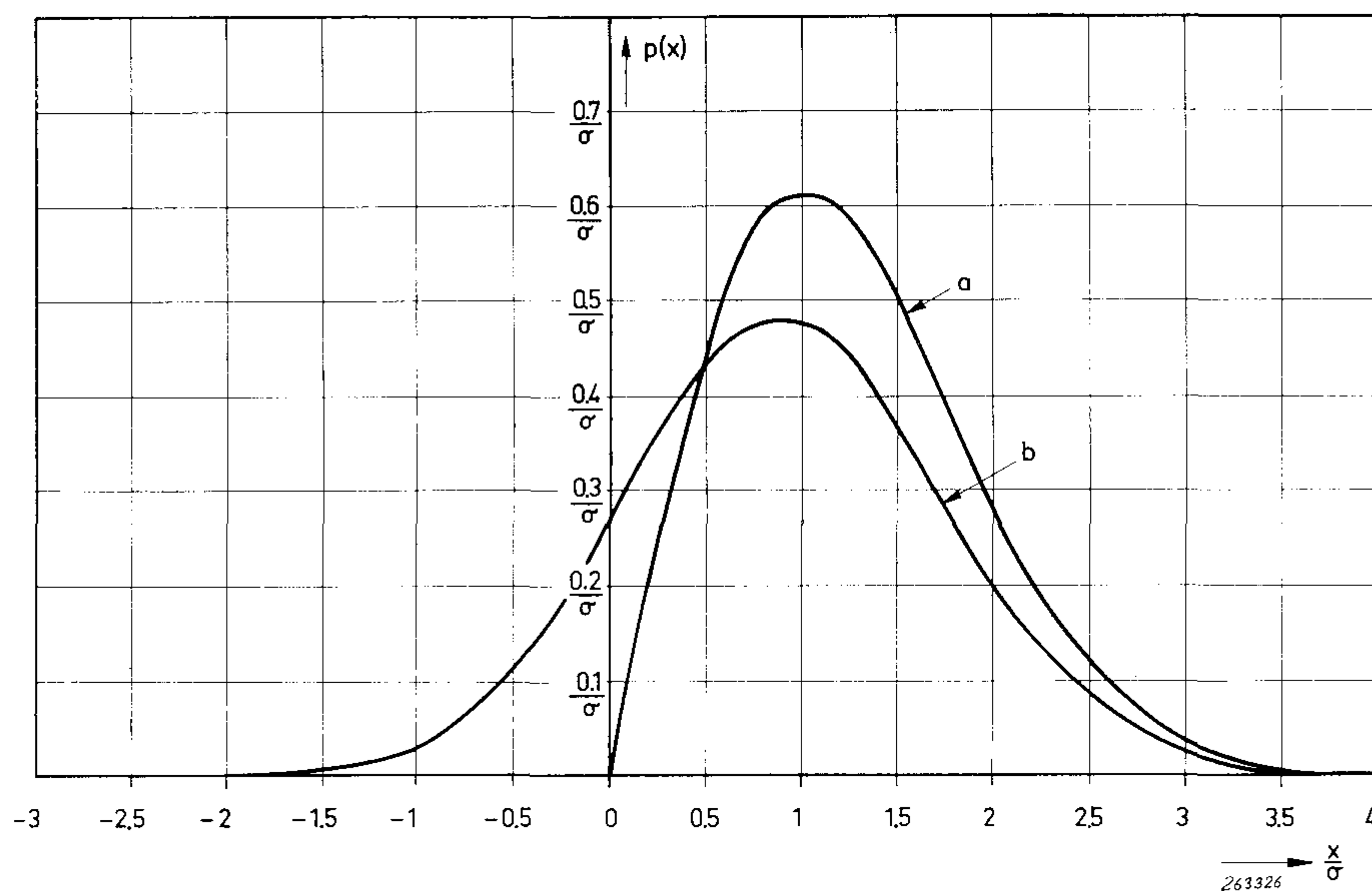


Fig. 1. Probability density curves for the distribution of noise maxima.  
a) Valid for an “infinitely narrow” band-pass filter (Rayleigh-distribution).  
b) Valid for a “flat” low-pass filter with infinitely sharp high frequency cut-off (Rice).

### General Theory of the Peak Distributions.

It has been shown by Rice a.o. that signals which exhibit Gaussian (normal) *instantaneous value* distribution can be represented by an infinite number of sine waves combined in random phase, independent of spectrum shape. However, the *peak values* will, to a great extent, be influenced by the spectrum shape. Rice found a general formula for the peak distribution as a function of spectrum shape as long as the circuits behave linearly in amplitude response i.e. as long as the above statement of Gaussian distributed instantaneous values holds true.

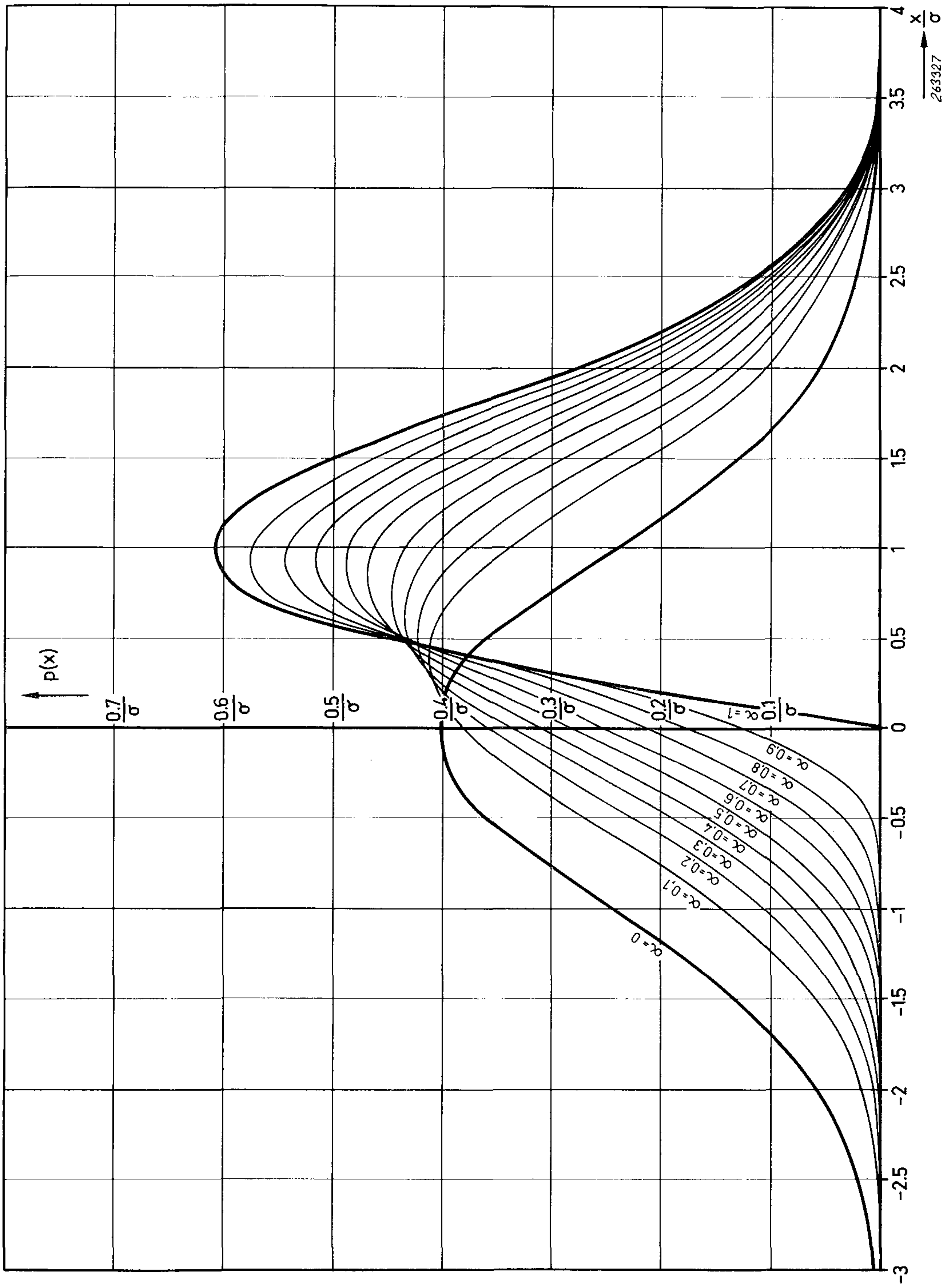


Fig. 2. Set of peak probability density curves with  $\alpha$  as parameter.



Actually the formula given by Rice consists of two additive terms, one which has a Gaussian character with zero as a mean, and one which has the character of a Rayleigh like distribution.

A slight transformation of Rice's original formula gives:

$$p(x) = \underbrace{\frac{\sqrt{1-\alpha}}{\sigma\sqrt{2\pi}} \cdot \exp\left[-\frac{x^2}{2\sigma^2(1-\alpha)}\right]}_{\text{"Gauss"-term}} + \underbrace{\frac{\sqrt{\alpha}}{2\sigma} \cdot \frac{x}{\sigma} \cdot \left[1 + \operatorname{erf}\left(\frac{x}{\sigma} \sqrt{\frac{\alpha}{2(1-\alpha)}}\right)\right]}_{\text{"Rayleigh"-like term}} \exp\left[-\frac{x^2}{2\sigma^2}\right]$$

In the formula:

$x$  = peak values of the signal.

$\sigma$  = r.m.s. value of the signal (standard deviation).

$\alpha$  = parameter, see Appendix, p. 30.

$\operatorname{erf}$  = error function.

$p(x)$  = probability density of  $x$ .

It can be seen that the relative importance of the two terms solely depends upon the value of  $\alpha$ . If  $\alpha = 0$  the peak distribution is truly Gaussian while if  $\alpha = 1$  the distribution is truly of the Rayleigh type. Therefore *the shape of the peak distribution curve will always lie between a Gaussian distribution and a Rayleigh distribution*. The factor  $\alpha$  depends on the spectrum shape and will be discussed in detail in the following. In Fig. 2 plots of the probability density

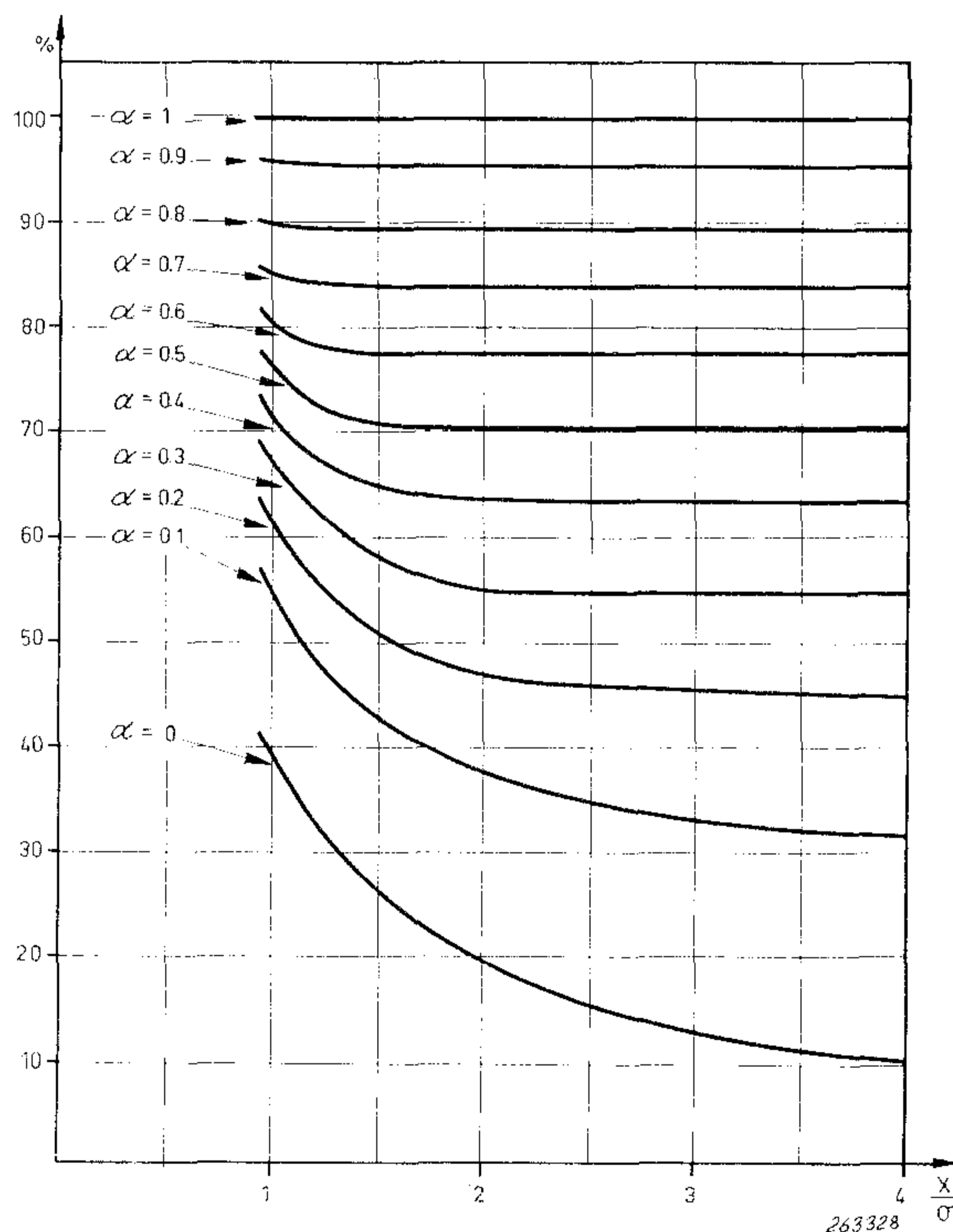


Fig. 3. The curves shown in Fig. 2 replotted in per cent of the true Rayleigh distribution.

function  $p(x)$  are given with  $\alpha$  as parameter, and Fig. 3 shows the same curves replotted in per cent of the true Rayleigh-distribution also with  $\alpha$  as parameter. It can be seen from Fig. 3 that the higher peak values always tend to show a Rayleigh like distribution (see also formula above) but the absolute probability density at these levels deviate from those of the Rayleigh distribution. The deviation from the Rayleigh distribution is due to the peaks and notches contained in each "main half cycle" of the noise signal, see Fig. 4 and the importance of the deviation must, in practical cases, be judged from this point of view.

To possibly aid such judgements being performed, typical signal wave forms will be shown together with the experimental results obtained in this article.

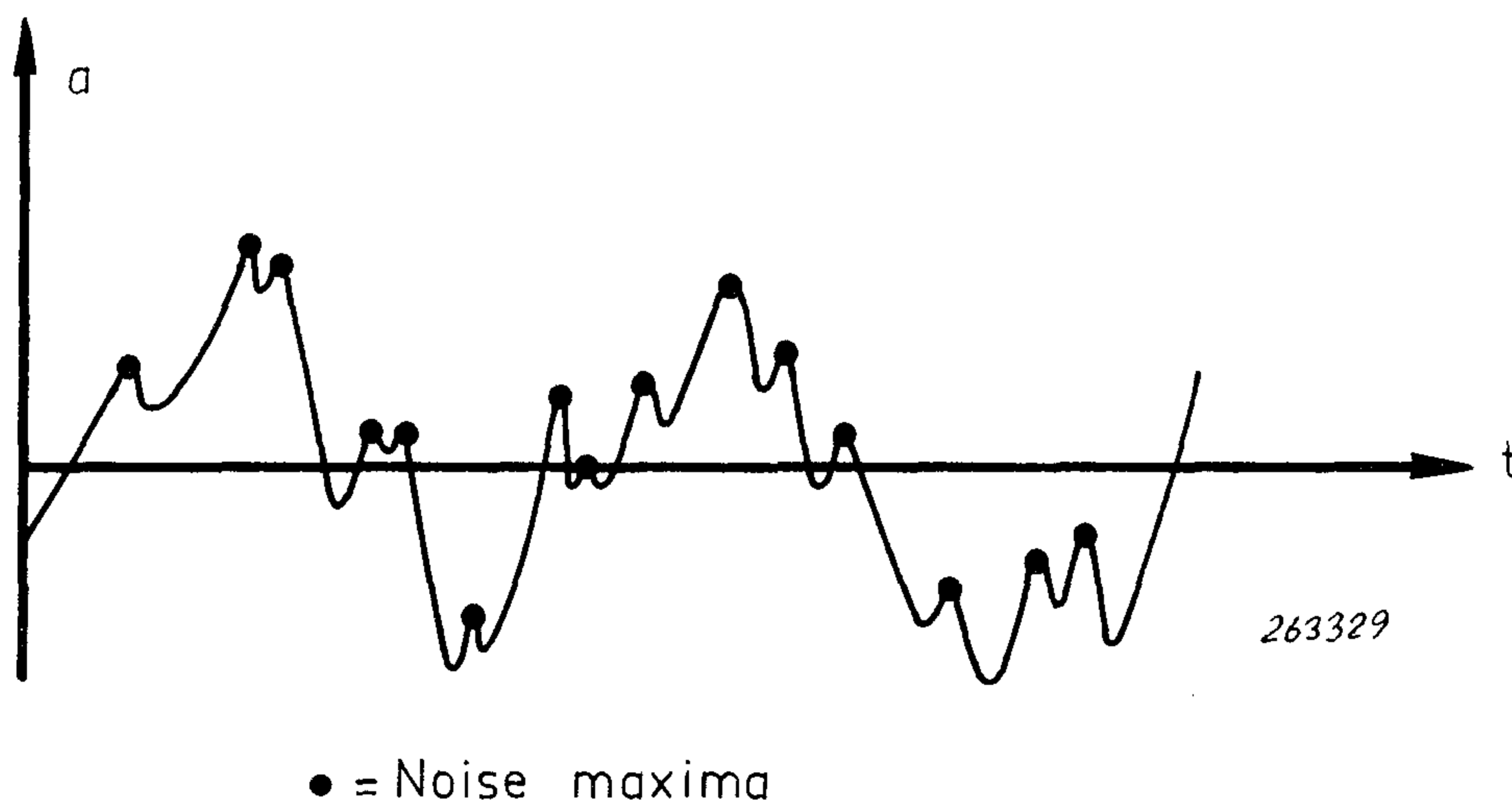


Fig. 4. Sketch illustrating the distribution of maxima in a sample of a wide band noise signal.

#### Types of Spectra Investigated.

The following types of spectra and "mechanical" systems have been investigated:

1. Spectra where the power spectral density decreases or increases with frequency at a constant rate between two "limiting" frequencies, see Fig. 5.
2. A system consisting of a spring and velocity dependent damping, (low-pass filter) Fig. 6.
3. Single degree of freedom systems Fig. 7 and "idealized" single degree of freedom systems.

The "idealization" is based upon energy-relations and it is shown that this kind of idealization is reasonable on account of the measured results. The "idealization" considerably simplifies the theoretical treatment of peak distributions in important practical cases.

4. Multi degree of freedom systems, Fig. 8.

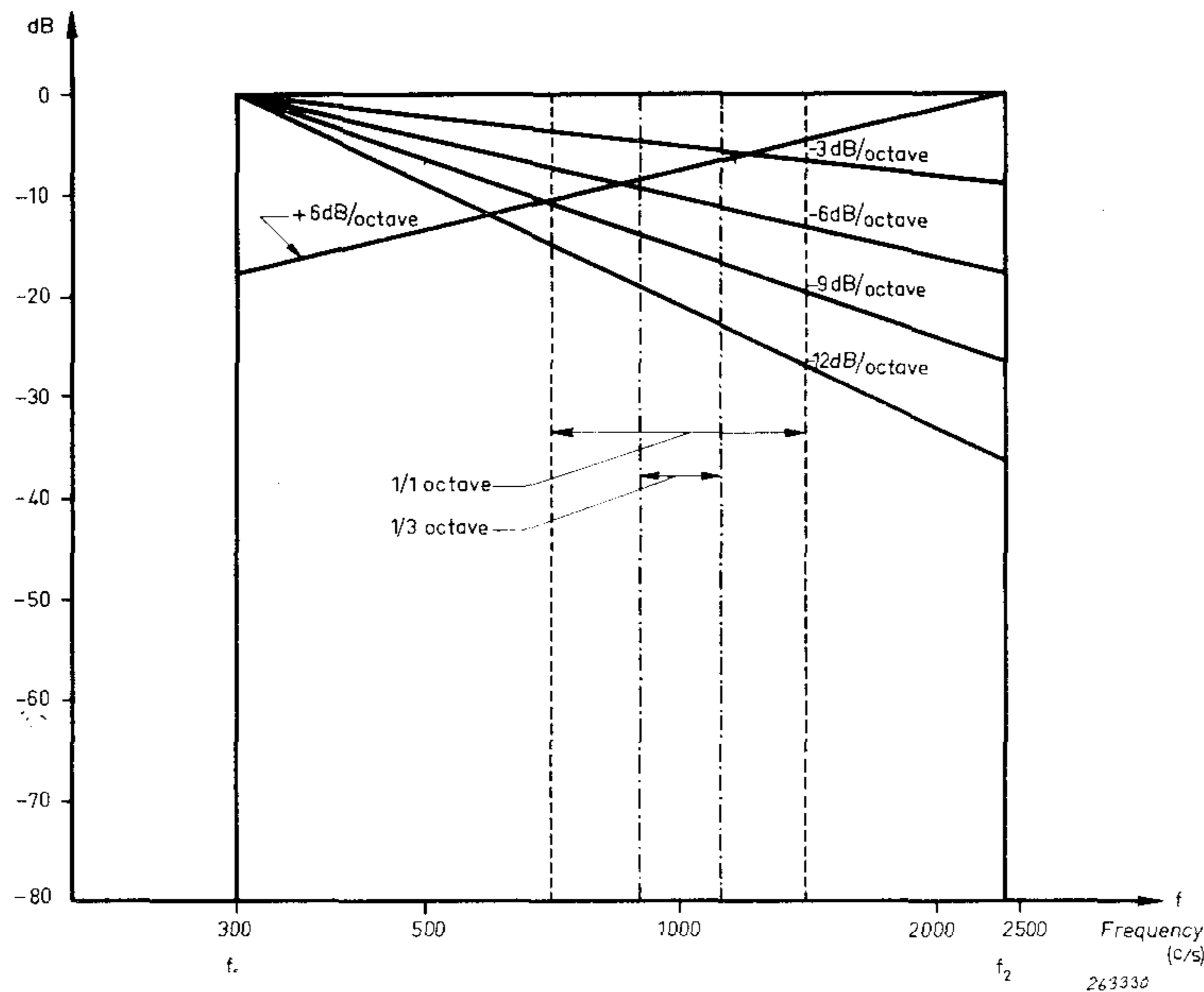


Fig. 5. Plots of the power spectral density vs. frequency for various "theoretical" noise spectra.

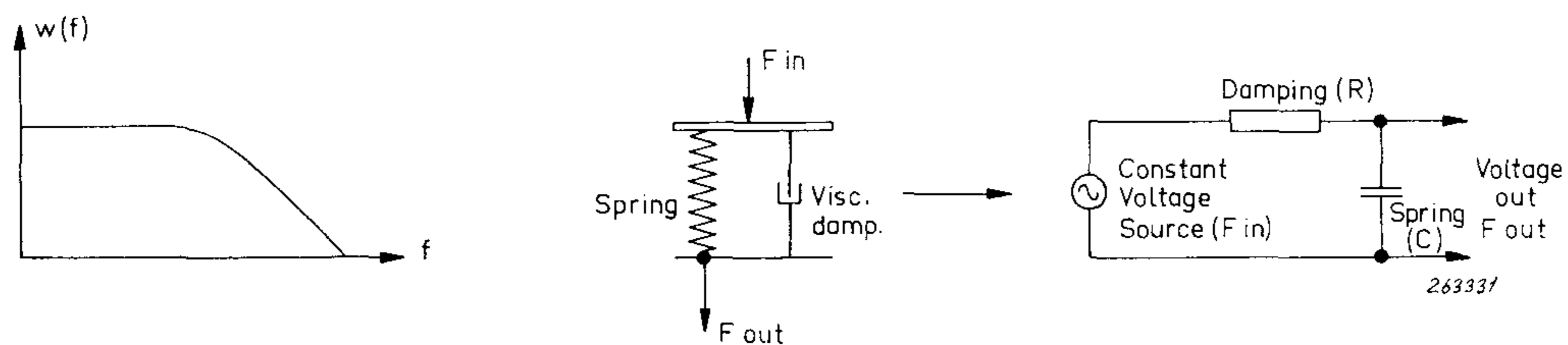


Fig. 6. Frequency response, "mechanical diagram" and electrical analogue circuit (impedance analogy) of a mechanical system consisting of a spring and viscous damping. The response plot shows the force measured on the spring when a constant, frequency independent force is applied to the complete system.

### Experimental Technique.

To verify the theoretical conclusions a special measuring arrangement was developed. It consists of a random noise generator (B & K Type 1402), a modified electronic counter, a variable DC supply and a true R.M.S. Voltmeter (B & K Type 2603). Use was also made of a band-pass filter set (B & K Type 1612) and a band-pass filter with very sharp cut-offs. Fig. 9 shows the basic set-up.

The counter was of a construction that made it possible to produce a voltage "window", Fig. 10. Furthermore the circuitry allowed the following conditions to be provided: When a signal voltage with a positive slope passed through the lower "end" of the "window" the counter was "made ready" to count. If the voltage then dropped below the "window" a count was registered. On the other hand, if the voltage increased and passed through the upper "end" of the "window" the counter was blocked until the

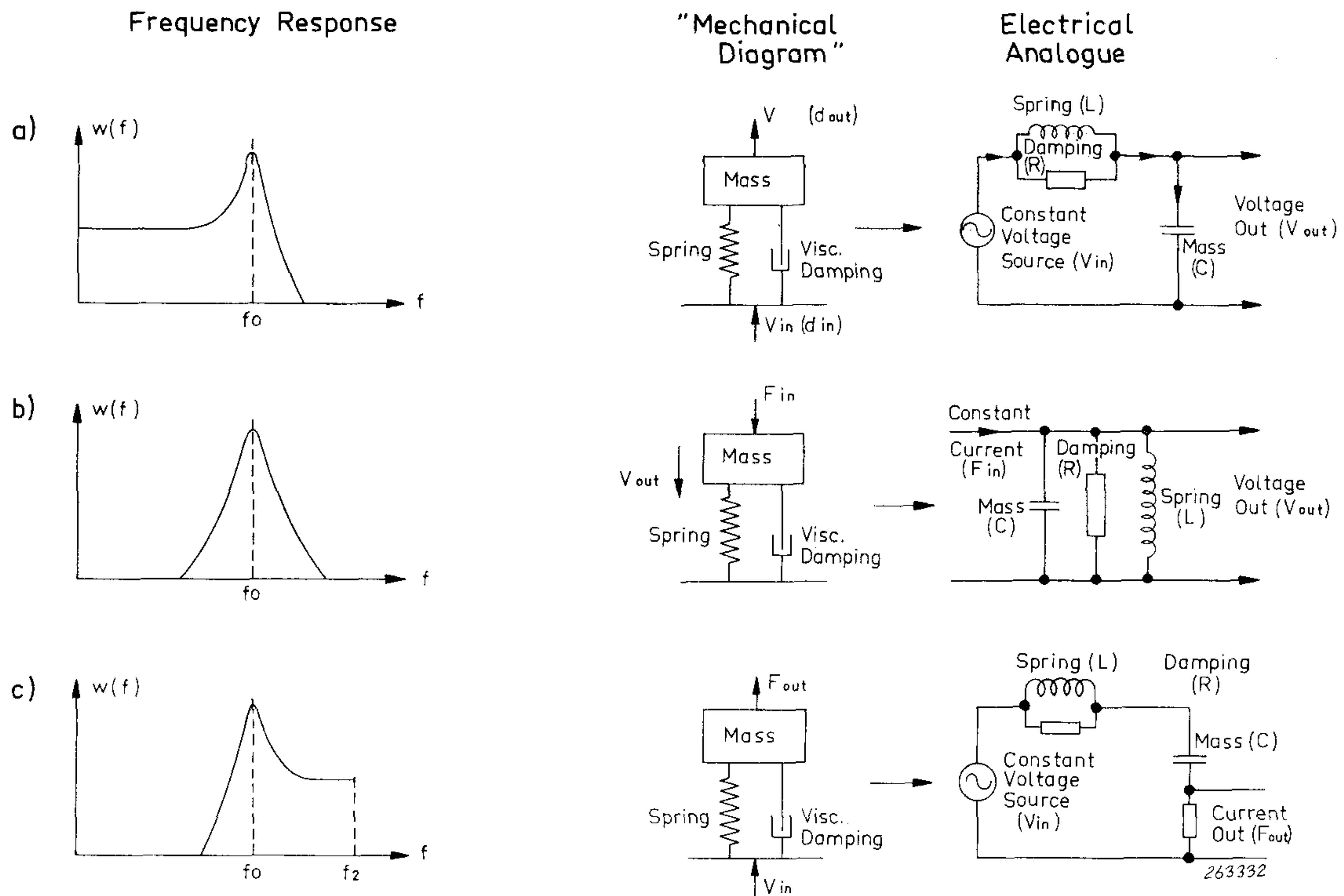


Fig. 7. Frequency response plots, "mechanical diagrams" and electrical analogue circuits of single degree freedom systems (mobility analogy). In the drawing are  $F =$  force,  $V =$  velocity,  $d =$  displacement and  $a =$  acceleration.

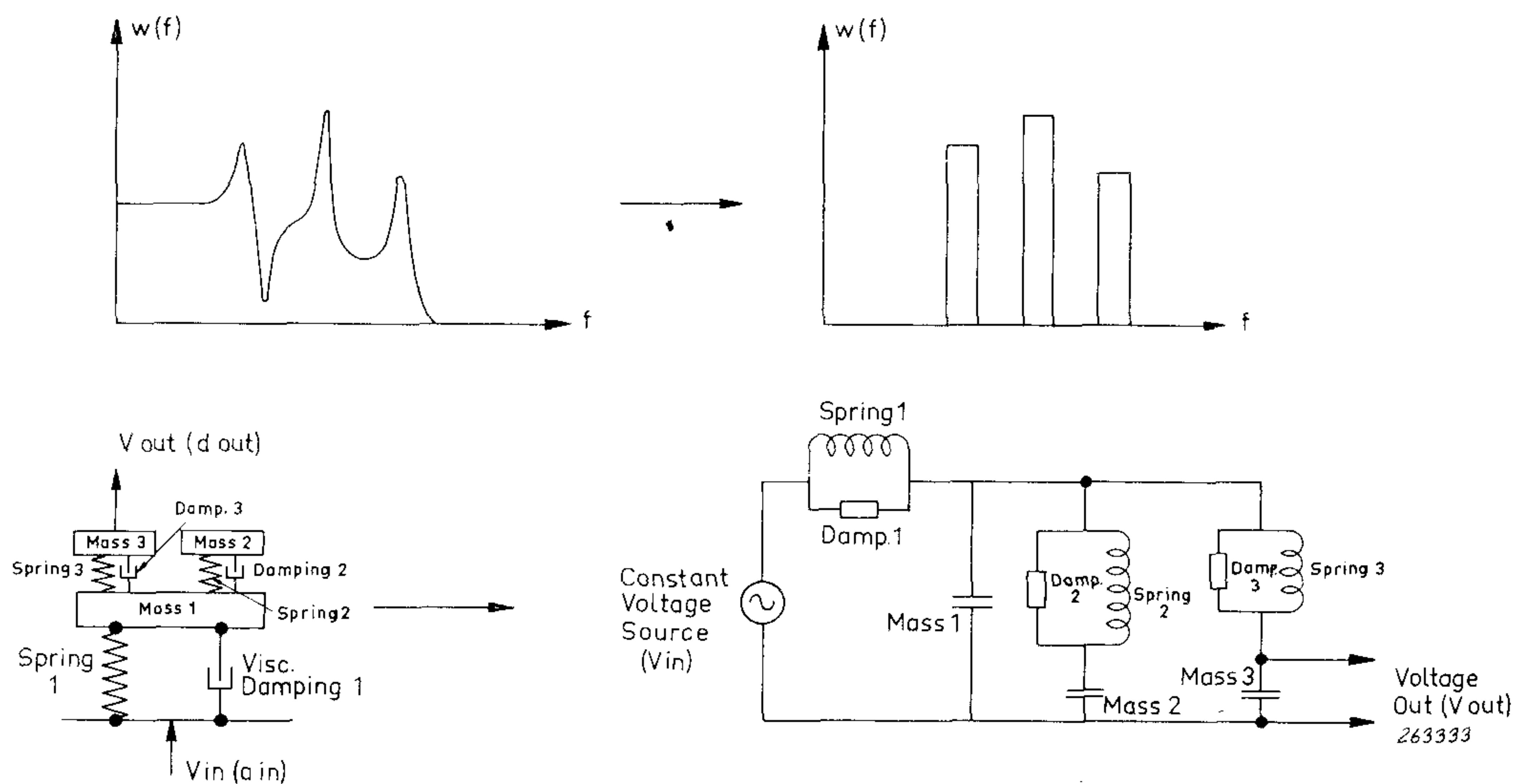


Fig. 8. Frequency response, "idealized" response, "mechanical" diagram and electrical analogue circuit (mobility analogy) of a multidegree of freedom system.

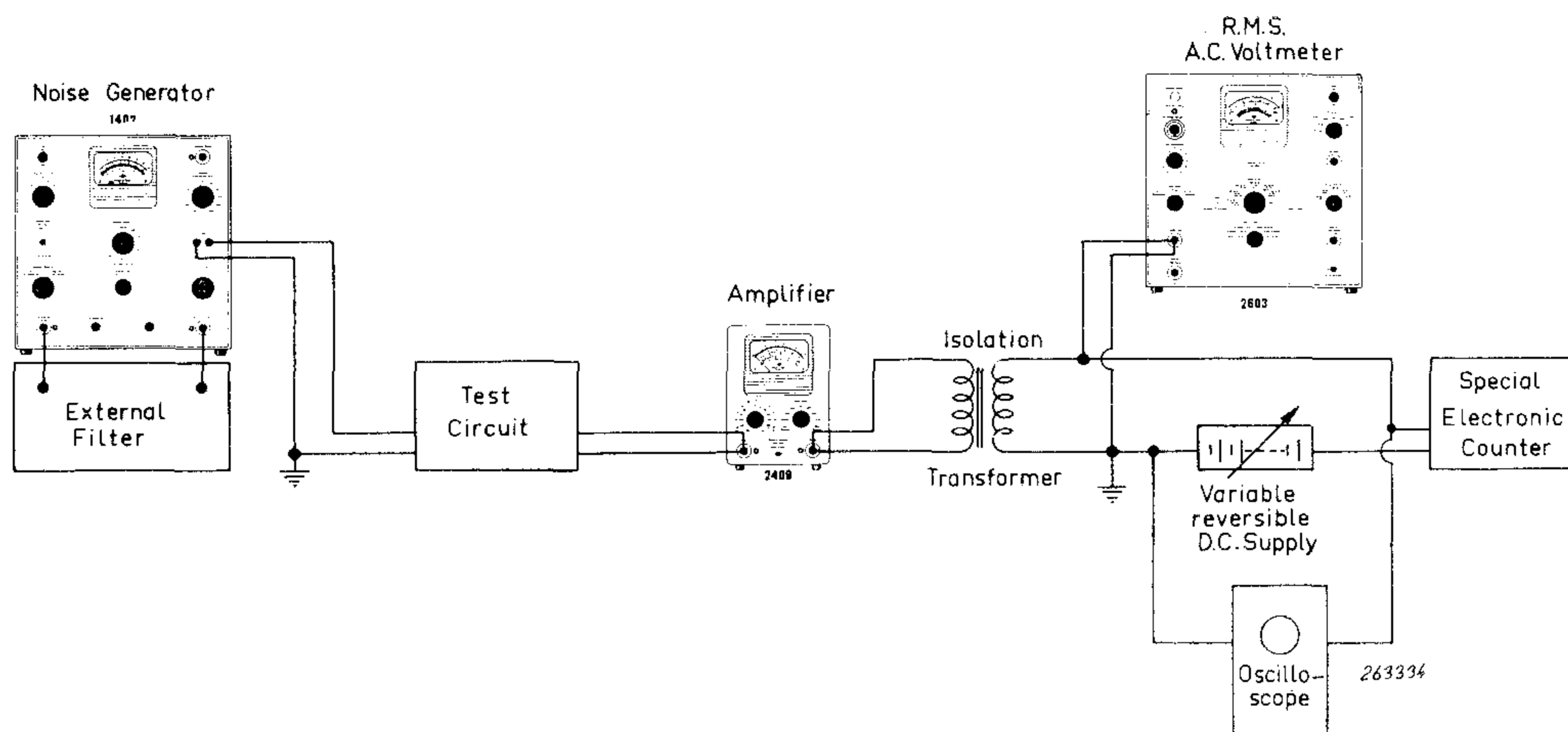


Fig. 9. Measuring arrangement used to determine experimentally the probability density curves of noise voltage maxima.

voltage again had dropped to a value below the lower “end” of the window. In this way a count was only registered if a voltage peak occurred within the limits of the “window”. Calibration was made with a sinusoidal signal and it was possible to keep the width of the window constant to within narrow tolerances during all the measurements. It can be seen from Fig. 10 that a combination of a peak and notch which lie within the window will not

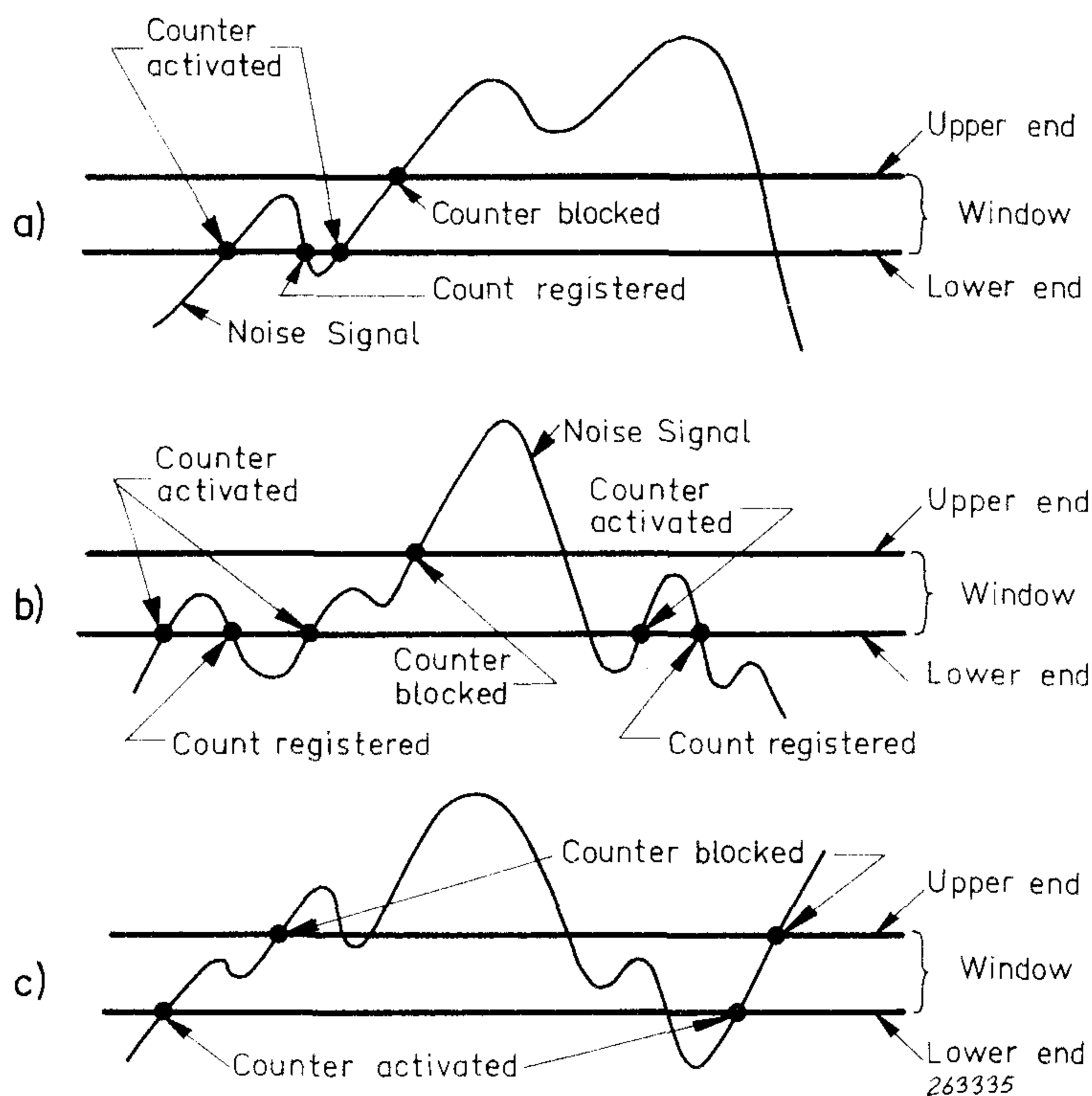


Fig. 10. Sketch illustrating the principle of operation of the arrangement shown in Fig. 9.

- a) One noise maximum is registered on the counter.
- b) Two noise maxima are registered.
- c) No noise maximum is registered.

be registered. When the window is chosen to be very narrow all but the rather insignificant peaks will be counted. The distinction between “significant” and “insignificant” peaks is rather difficult to draw up sharply, but it will be shown later that a very useful kind of distinction may be made on an energy-basis. By moving the “window” relative to the signal the number of peaks occurring in certain time intervals (measuring time), and at various signal levels can be determined. For most of the measurements reported here a “window” width of  $0.2 \sigma$  was used and the measuring time was chosen to be 2 min. The frequency range in which measurements were made was from some 300 c/s to around 2400 c/s.

### **The Peak Distributions of some Theoretical Spectra.**

In this section, a special type of frequency spectra, not likely to be exactly met in practice, is dealt with. However, some important conclusions may be drawn from these investigations which are used later in the work. The spectra are of the type shown in Fig. 5 and the power spectral density inside the “pass-band” can be written:

$$w(f) = c \times f^n$$

where  $c$  is a constant,  $f$  = frequency and  $n$  an exponent that can be positive, negative or zero. The full mathematical treatment of the problem will not be given here, but it should be mentioned that it is necessary to divide the problem into several “cases”, so that no one general formula can be given which covers all values of  $n$ . Fig. 11 shows the theoretically derived curves for  $\alpha$  as a function of  $n$ , with the ratio between the limiting frequencies

( $f_1$  and  $f_2$ ) as parameter. It can be seen that for  $\frac{f_2}{f_1}$  smaller than around 2 (1/1 octave bandwidth) the lowest  $\alpha$ -value is obtained in a range of  $n = 0$  to  $n = -6$  and that  $\alpha$  is practically constant within this range. Also the lowest  $\alpha$ -value is approximately 0.86 which, from the curves shown in Fig. 3, gives a Rayleigh like peak distribution for peak values higher than some  $1.25 \sigma$ . Considering this the following conclusion may be drawn:

*The shape of the “filter” characteristic inside the pass-band of a resonant filter system (single degree-of-freedom system) narrower than some 1/1 octave does not change the distribution of important peaks to any appreciable extent, and may thus, in practical cases, be approximated by means of a “box” containing roughly the same amount of energy, i.e. having the same R.M.S.-value ( $\sigma$ ) as the original noise.*

On the other hand, if the band considered is considerably greater than 1/1 octave ( $\frac{f_2}{f_1} \gg 2$ ) the slope of the spectrum inside the band will theoretically

influence the peak distribution to quite an extent. If, for example  $\frac{f_2}{f_1}$  is of the order of 25 or higher and the slope of the spectrum is some  $-9$  dB/octave ( $n = 3$ ), the theoretical peak distribution will be almost Gaussian ( $\alpha = 0$ ) see Fig. 11. Now, what does it mean physically when the peak distribution

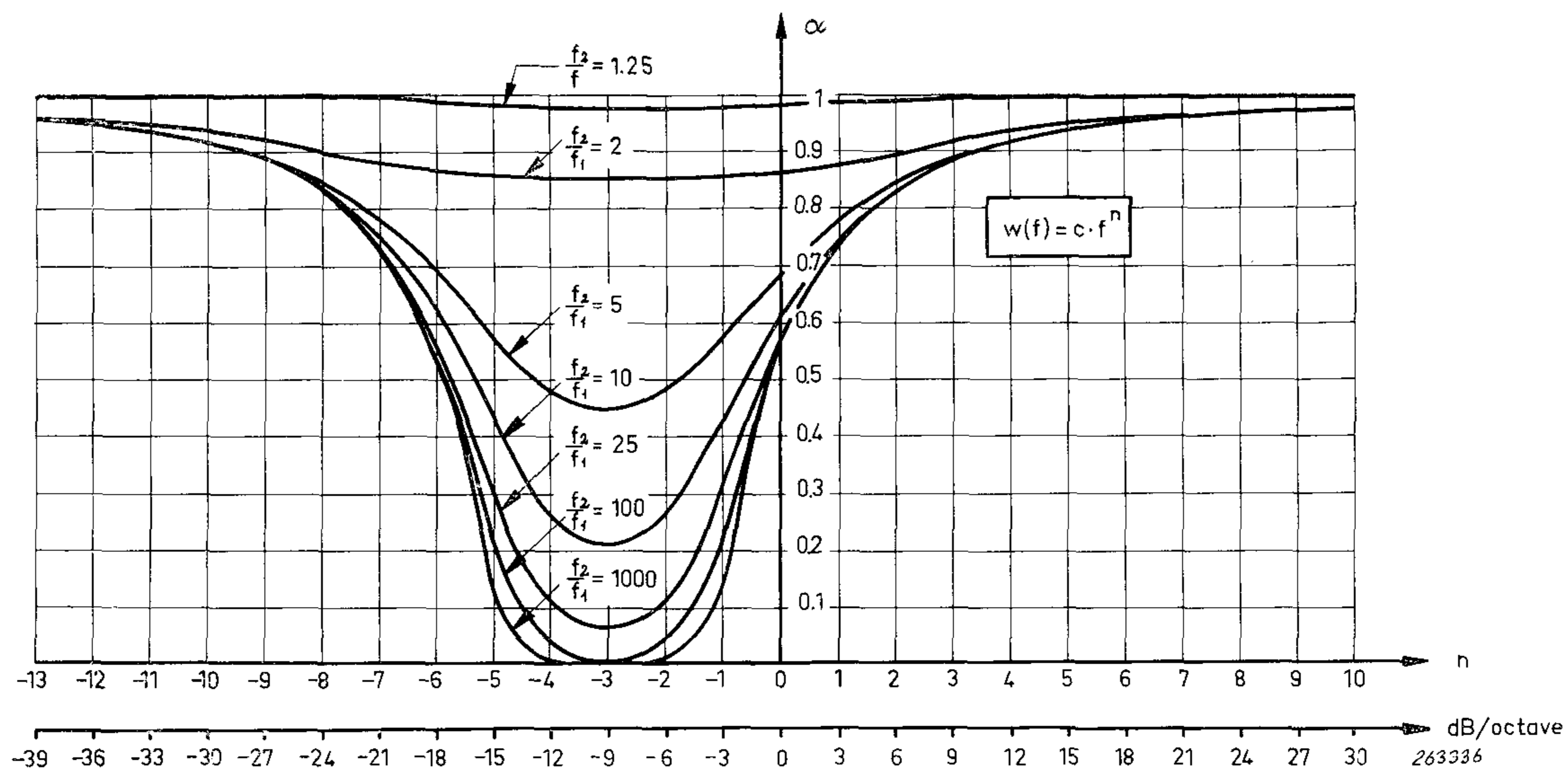
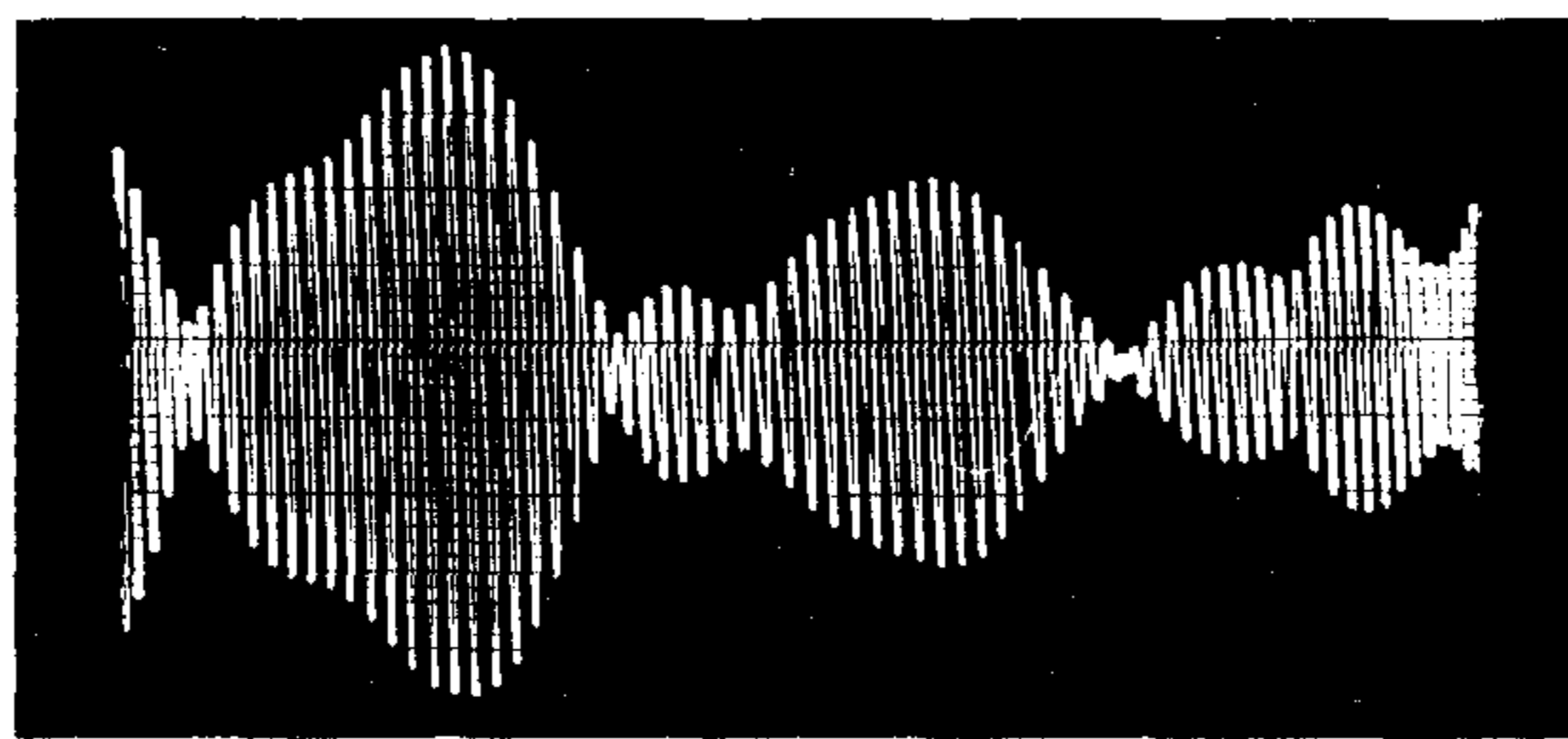
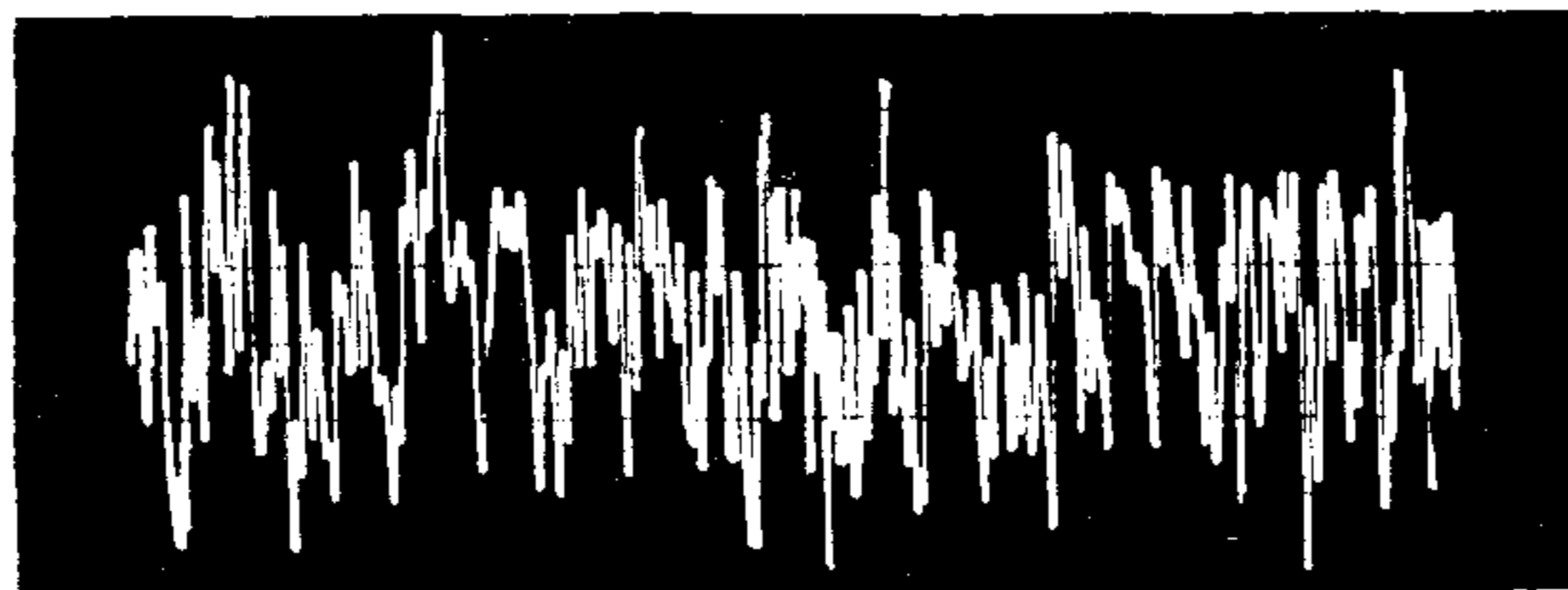


Fig. 11. Curves showing how the factor,  $\alpha$ , varies with the exponent,  $n$ , (spectrum slope) for various ratios .

approaches a Gaussian shape? This can be explained on the basis of Fig. 12. Here two signals are shown, one which has a “true” Rayleigh distribution of the peaks (narrow band noise) and one which has a Gaussian type peak distribution. It is clearly noticed that to obtain a *true* Rayleigh distribution only *one* noise maximum (or minimum) occur between two succeeding zero crossings of the signal, while in the case of a Gaussian type peak distribution a number of “smaller” noise maxima (and minima) occur between the zeros. When the signal being studied is derived from mechanical vibrations of a part or structure and the difference between a maximum and the succeeding minimum becomes greater the existence of these “smaller” peaks and notches



a)



b)

Fig. 12. Two typical noise signals:

a) Narrow band noise

b) Wide band noise

Note the difference in the distribution of maxima.

may become important. In this case they will cause "extra" losses to be induced in the already prestressed material and may thus to a certain extent, contribute to possible malfunction of the part or structure due to fatigue. It may therefore be assumed that in the case of vibration signals these types of peaks and notches may have to be taken into account when predicting the fatigue life of the part.

Some experiments have been made in an attempt to check the theoretically predicted peak distributions discussed in the preceding text. The measuring arrangement sketched in Fig. 9 was used and the output signal from the Random Noise Generator Type 1402 was shaped so that spectra of the type shown in Fig. 5 were obtained.

The 1/3 and 1/1 octave spectra were produced by connecting a Band-pass Filter Set Type 1612, as "External Filter", to the generator and making use of the built-in  $-3$  dB/octave condition as well as a simple R-C-circuit. In the case of the wide-band output signals the Band-Pass Filter Set Type 1612 was substituted by a special band pass filter with sharp cut-offs at approximately 300 c/s and 2.4 kc/s. With the above mentioned R-C-circuit connected across the output of the Generator, a spectrum with a slope of  $-6$  dB/octave is obtained, and combining this with the built-in  $-3$  dB/octave condition, spectra with slopes of  $-3$  dB/octave,  $-6$  dB/octave and  $-9$  dB/octave can be readily produced. Also by using a second R-C-circuit a spectrum slope of  $-12$  dB/octave was obtained.

Fig. 13 shows the resulting peak distributions measured on the 1/3 and 1/1 octave noise bands. It was not possible, within the measuring accuracy, to state any difference in distribution whether the spectrum inside the pass-band was flat or had a slope of  $-9$  dB/octave, and the results seem to closely follow the ones theoretically predicted.

The center frequency, of the noise bands used in the experiments, was 1000 c/s.

The measurements on the wide band signal were considerably more difficult to perform in that here, the "small" peaks and notches play an important role, and the width of the measuring "window" is therefore more critical. A "window" width of  $0.2 \sigma$  was chosen on the basis of the following considerations:

1. Succeeding peaks and notches inside  $0.2 \sigma$  will presumably be of little practical interest, and
2. With the equipment available, difficulties arose in keeping the instrumentation strictly linear up to  $4 \sigma$ -values if a narrower "window" was employed.

To obtain a fairly well defined  $\frac{f_2}{f_1}$ -ratio the afore mentioned special band-pass filter with very sharp cut-offs was designed, and inserted as "External Filter" in the Noise Generator.

A number of peak probability density curves were now measured for various spectrum slopes. The results are given in Fig. 14 where certain theoretical



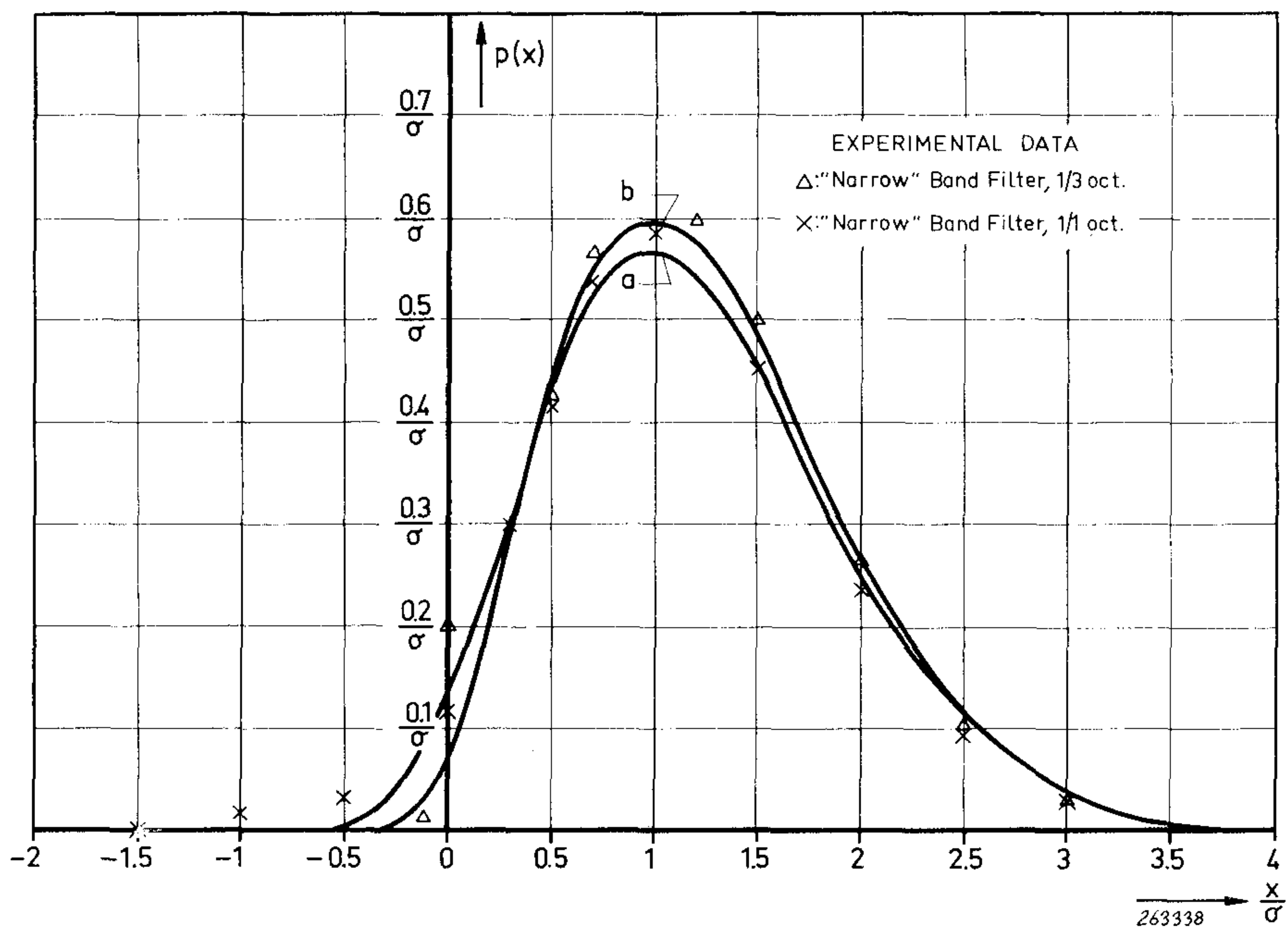


Fig. 13. Some experimental results:

- a) Probability density curve for the distribution of maxima in a 1/1 octave band of noise.
- b) Probability density curve for the distribution of maxima in a 1/3 octave band of noise.

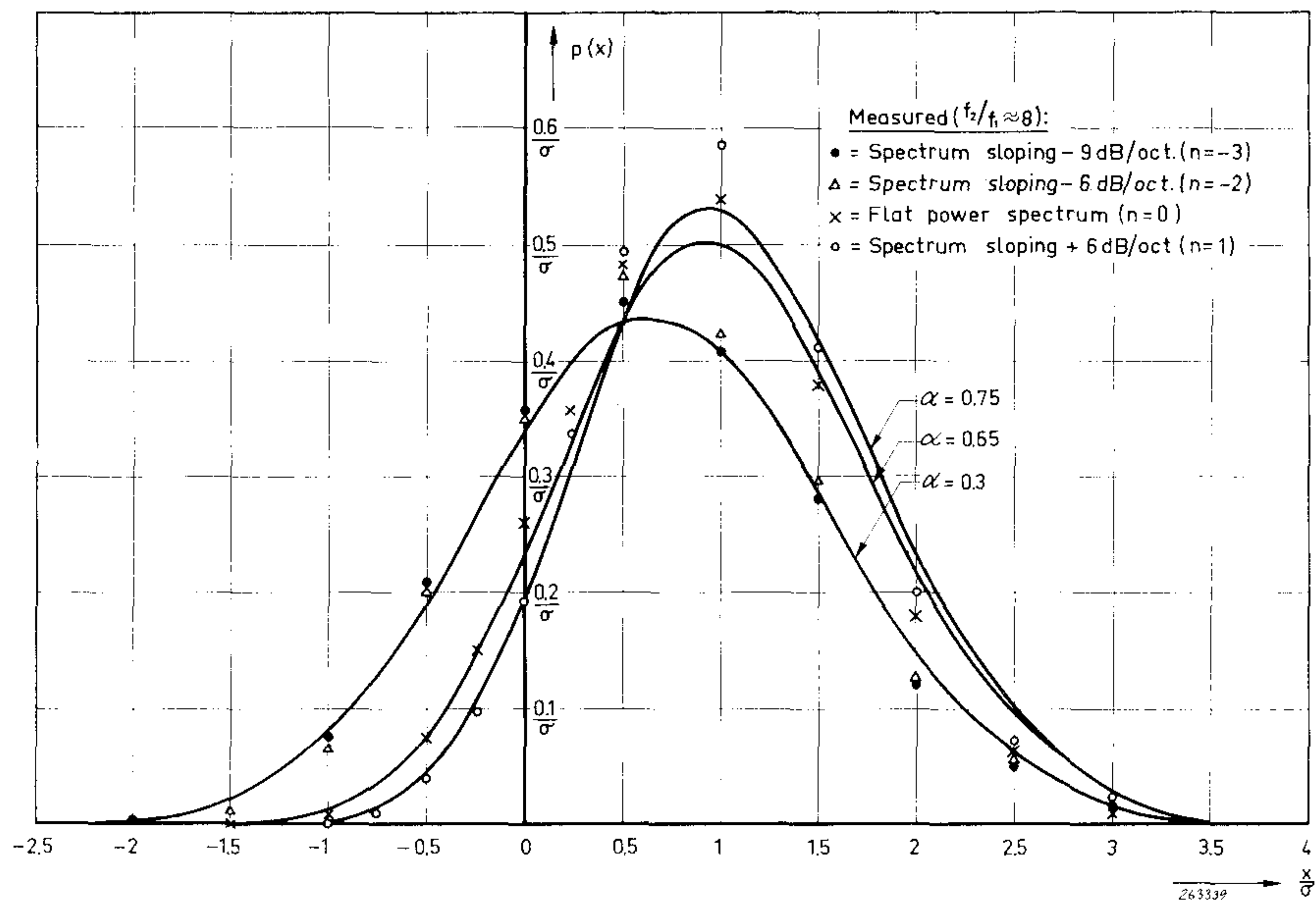


Fig. 14. Probability density curves for the occurrence of maxima in a wide-band ( $\frac{f_2}{f_1} \sim 8$ ) noise signal. Comparison of theoretical and measured results.

curves are also plotted. These curves correspond to  $\alpha$ -values of 0.3, 0.65, and 0.75, and by consulting Fig. 11, it can be seen that they represent the theoretical probability density curves expected for an  $\frac{f_2}{f_1}$ -ratio of around 8.

It should be mentioned here that the deviation between the measured results and the theoretically predicted ones is most likely to be due to read-out, and meter errors in the measuring instruments. (A very small error in the r.m.s. value of the noise signal relative to the DC voltage setting the "window" level results in considerable "deformation" of the probability density curve).

The difference in probability density curve between the signal with a spectrum slope of  $-6$  dB/octave and that corresponding to a slope of  $-9$  dB/octave is rather insignificant. This also agrees very well with the theoretical results of Fig. 11.

In Fig. 15 are shown some typical wave-shapes obtained for various spectrum slopes and  $\frac{f_2}{f_1} \simeq 8$ . Fig. 15 (a) shows the case where the spectrum slope is  $+6$  dB/octave ( $n = 2$ ), while in Fig. 15 (b) the signal frequency spectrum was "flat". With a spectrum slope of  $-6$  dB/octave a signal of the type shown in Fig. 15 (c) was obtained. Finally Fig. 15 (d) indicates the wave-shape when the spectrum slope was  $-9$  dB/octave. The change from a typical "high frequency signal" to a typical "low frequency signal" as a function of spectrum slope is clearly noticed. Also note the change in signal "characteristic". While the signal shown in Fig. 15 (a) has an almost Rayleigh (narrow band) character the signal in Fig. 15 (d) shows a number of small peaks and notches at various levels.

In the following, extensive use will be made of the experimental results obtained here with regard to the effect of spectrum slopes upon the peak distribution.

### **Low-pass "Filter".**

The shape of the theoretical peak distribution for an ideal (boxshaped) low-pass filter has been given by Rice and corresponds to  $\alpha = \frac{5}{9}$ . If on the other hand, exact calculations on an actual low-pass filter of the type shown in Fig. 6 and which is equivalent to a spring with velocity type damping are carried out, one comes to the result that when a true "white" noise signal ( $f_x \rightarrow \infty$ ) is impressed upon the system the peak distribution will be Gaussian. This is also to be expected from the results obtained with the "theoretical spectra" above, in that then  $\frac{f_2}{f_1} \rightarrow \infty$  and the spectrum slope is  $-6$  dB/octave ( $n = -2$ ) see also Fig. 11. Physically the Gaussian shape is due to the very small peaks and notches caused by the high frequencies being considered by the exact mathematical theory. These peaks and notches may however, be of little, if any, practical importance. Mathematically the case reveals itself in that some of the integrals concerned do not converge. Rice, in his original

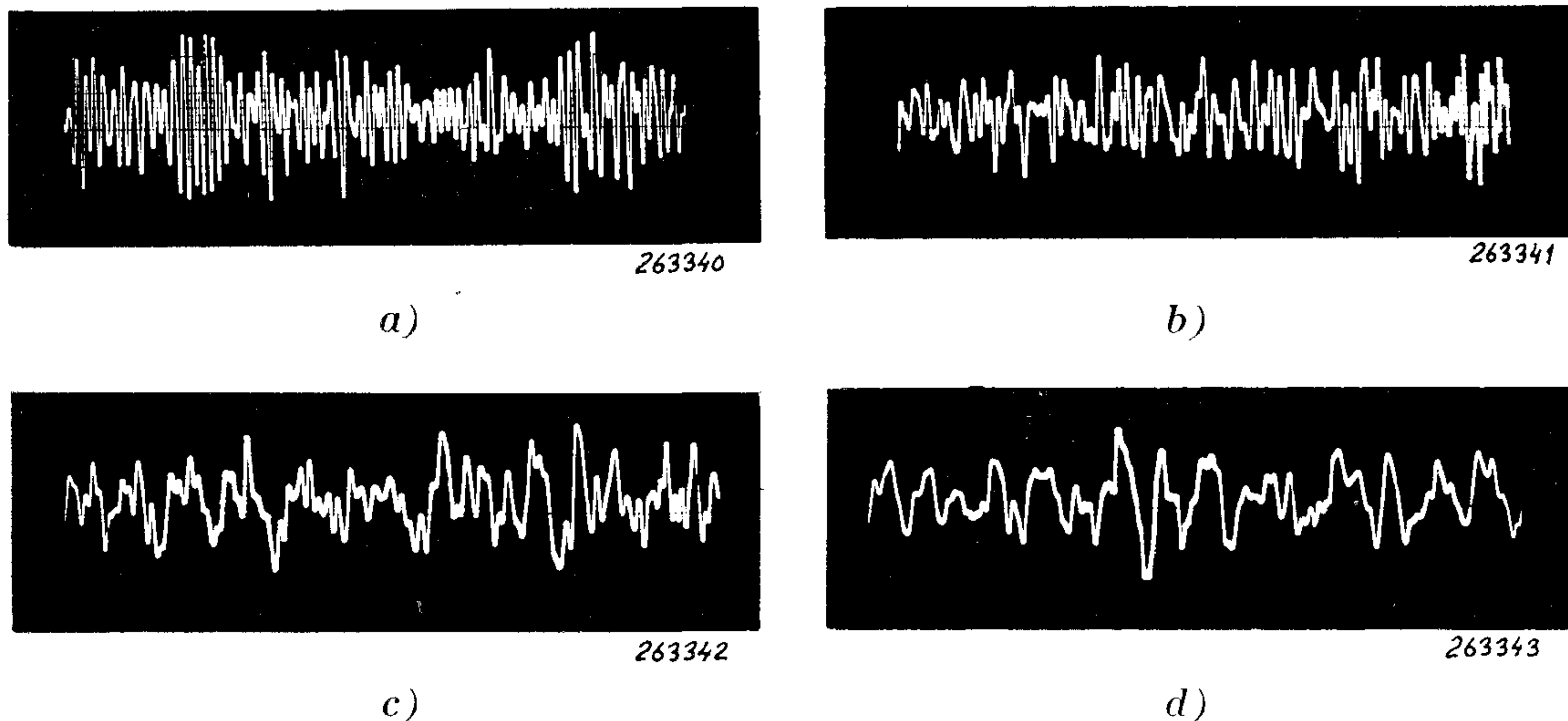


Fig. 15. Samples of wide-band ( $\frac{f_2}{f_1} \sim 8$ ) noise signals:

- a) Noise spectrum sloping  $+ 6$  dB/octave ( $n = 2$ ).
- b) Flat (constant power spectral density) noise spectrum ( $n = 0$ ).
- c) Noise spectrum sloping  $- 6$  dB/octave ( $n = -2$ ).
- d) Noise spectrum sloping  $- 9$  dB/octave ( $n = -3$ ).

work also points this out and discusses briefly the case of the R-C-circuit. Some calculations have been made where a sharp cut-off was introduced at a frequency,  $f_x$ , above the R-C-cut-off frequency,  $f_0 = \frac{1}{2\pi RC}$ , and a curve of  $\alpha$  vs. the ratio  $f_x/f_0$  is shown in Fig. 16. Measurements have also been made in an attempt to check the curve up to  $f_x/f_0$  values of around 8 and the correlation was quite satisfactory, Fig. 17.

When  $f_x/f_0$  becomes greater, the high frequency peaks seem to be of such small magnitudes that they are outside the range of the measuring equipment, and they may then presumably also in practical cases be neglected.

### Single Degree of Freedom Systems.

A single degree-of-freedom system may consist of a mass, a spring and some sort of damping. In the general differential equation for these types of systems the damping is normally assumed to be of the viscous type (velocity dependent), and the system can be simulated by an electrical R-L-C-circuit. The actual configuration of the analogue circuit depends upon whether it is desired to know the acceleration, velocity or displacement of the responses and what type of forcing signal is used (acceleration, velocity or displacement).

The frequency response of the signal can then be one of the three types shown in Fig. 7, and the distribution of the peaks in all three cases will be considered in the following.

Again exact calculation of the peak-distribution (limits of integration 0 and  $\infty$ ) reveals that they should theoretically be of a Gaussian type in the case of

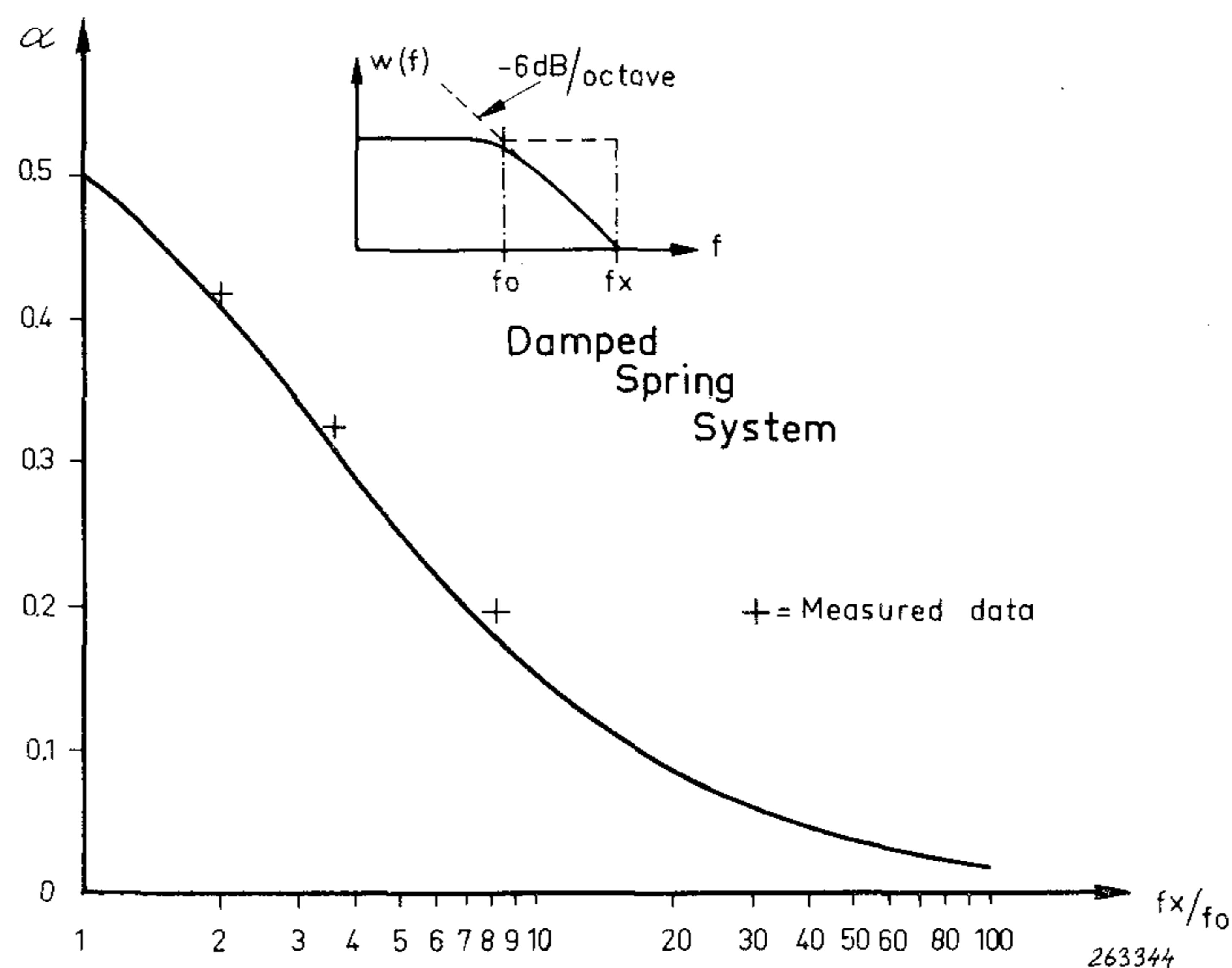


Fig. 16. Curve of  $\alpha$  vs.  $f_x/f_o$  for an R-C-type low-pass filter. Exact theoretically calculated curve is here compared with actually measured results (+).

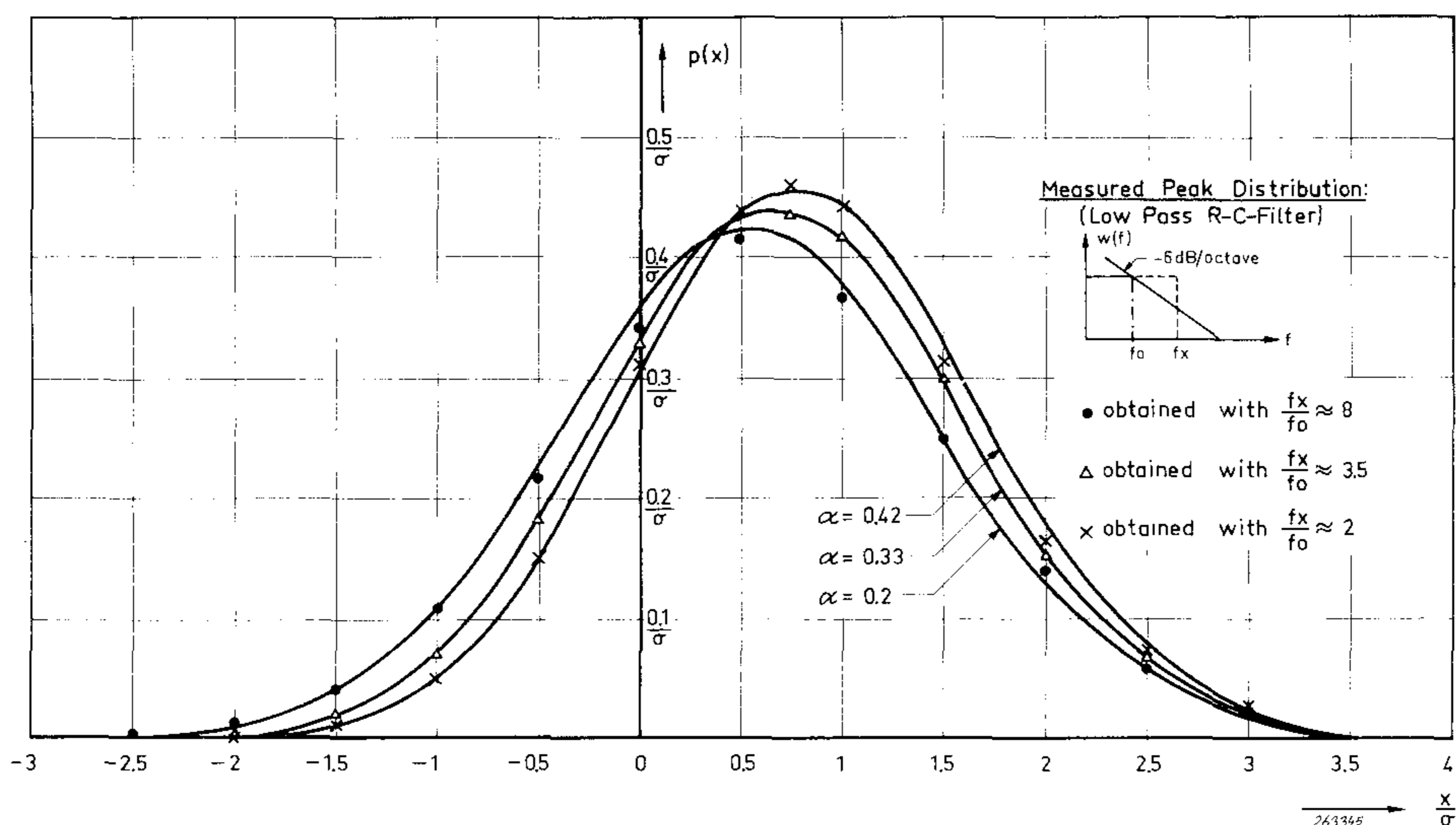


Fig. 17. Determination of  $\alpha$  from measured peak probability density curves for a damped spring system (R-C-circuit). See also Fig. 16.

spectra of the types shown in Fig. 7 (a) and (b) while in the case of Fig. 7 (c) the "limiting" case is  $\alpha = \frac{5}{9}$ .

This is in contradiction to practical experience where, for a reasonably high Q-value in the system, an almost ideal Rayleigh-distribution is found for the spectrum shape Fig. 7 (a). Also when looking at the signal on the screen of an oscilloscope it has, in this case, the distinct character of a narrow band noise signal even when the forcing spectrum is "white" up to some  $f_x/f_o = 40$ . The explanation for the difference between the results calculated from the exact mathematical theory and practical experience may also in this case, be

found in the existence of infinitely small high frequency peaks and notches. Considering, however, that by far the greatest part of the spectrum energy is contained in the resonance peak, it should be possible to approximate the type of spectrum shown in Fig. 7 (a) and (b) with a box-type spectrum containing the same amount of energy centered around the resonance frequency. (Confer also "The Peak Distribution of some Theoretical Spectra", p. 13). The top of the "box" should be equal to the maximum resonant response and the width of the "box" would be  $\frac{\pi}{2}$  times the  $-3$  dB bandwidth of the resonance, see also Fig. 18. \*)

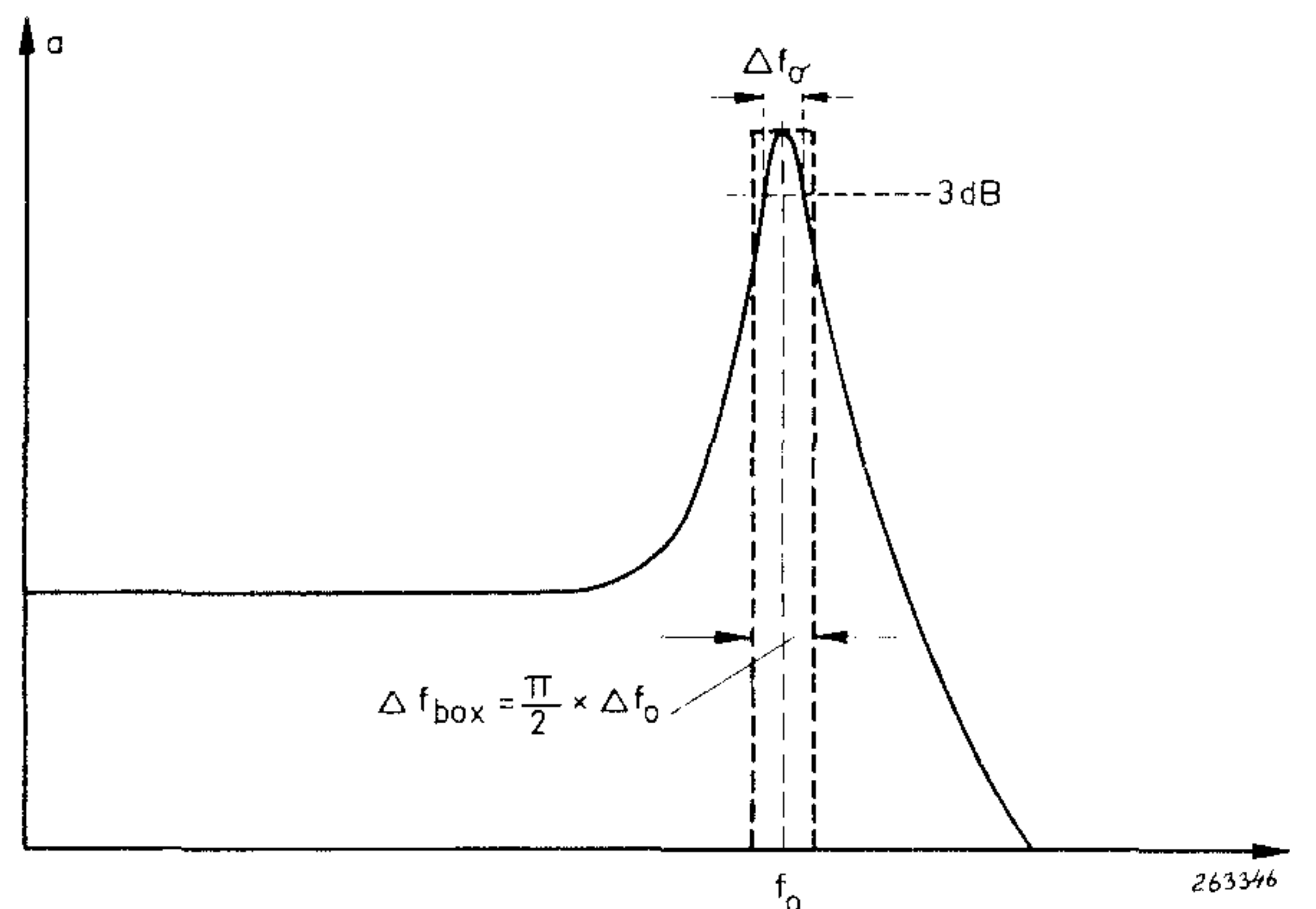


Fig. 18. Sketch showing how the frequency response of a single degree of freedom system is transformed into a "box" containing the same amount of energy.

To investigate the validity of the "box"-approximation a number of measurements have been made. The results of these are shown in Fig. 19 where the measured peak distributions are compared to the distributions calculated from the equivalent "box"-approximation for various Q-values of the system. It can be seen that even for Q-values as low as  $Q = 2$  the approximation is quite good in cases where the spectrum "end-slope" towards higher frequencies is  $-12$  dB/octave. When a spectrum of the type shown in Fig. 7 (b) is being considered the "box"-approximation can only be used when the Q-value of the system is considerably higher than in the case of Fig. 18 (or

\*) The RMS-value for the resonant system is:

$$\sigma_{\text{res}} = \sqrt{\frac{\pi \times w(f_i) \times f_0 \times Q}{2}} = \sqrt{\frac{\pi \times w(f_i) \times Q^2 \times \Delta f_r}{2}}$$

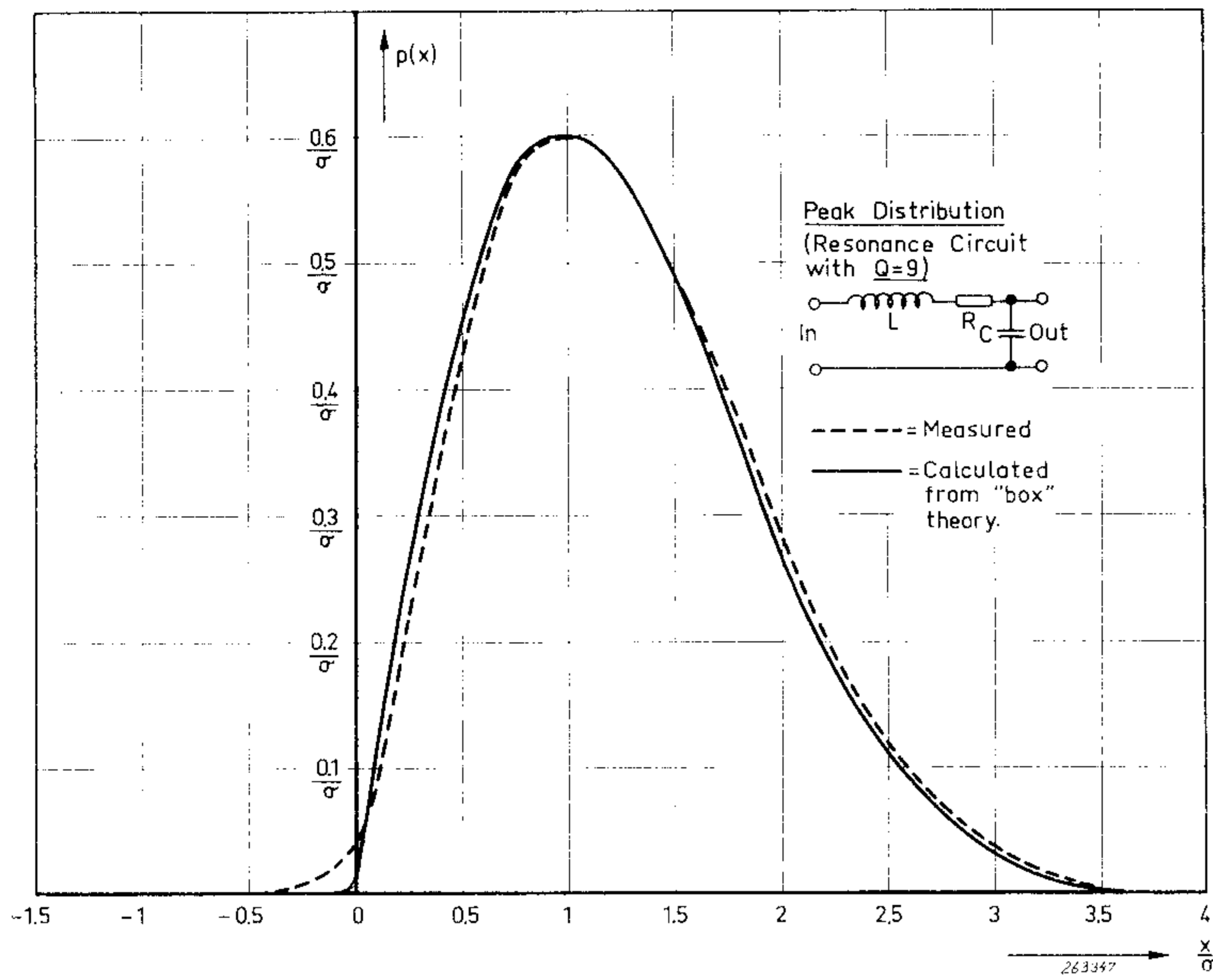
Where  $w(f_i)$  is the input power spectral density,  $f_0$  = resonance frequency,  $Q$  = resonant amplification factor of the system and  $\Delta f_r$  =  $-3$  dB resonance bandwidth.

The RMS-value of the equivalent "box-filter" is:

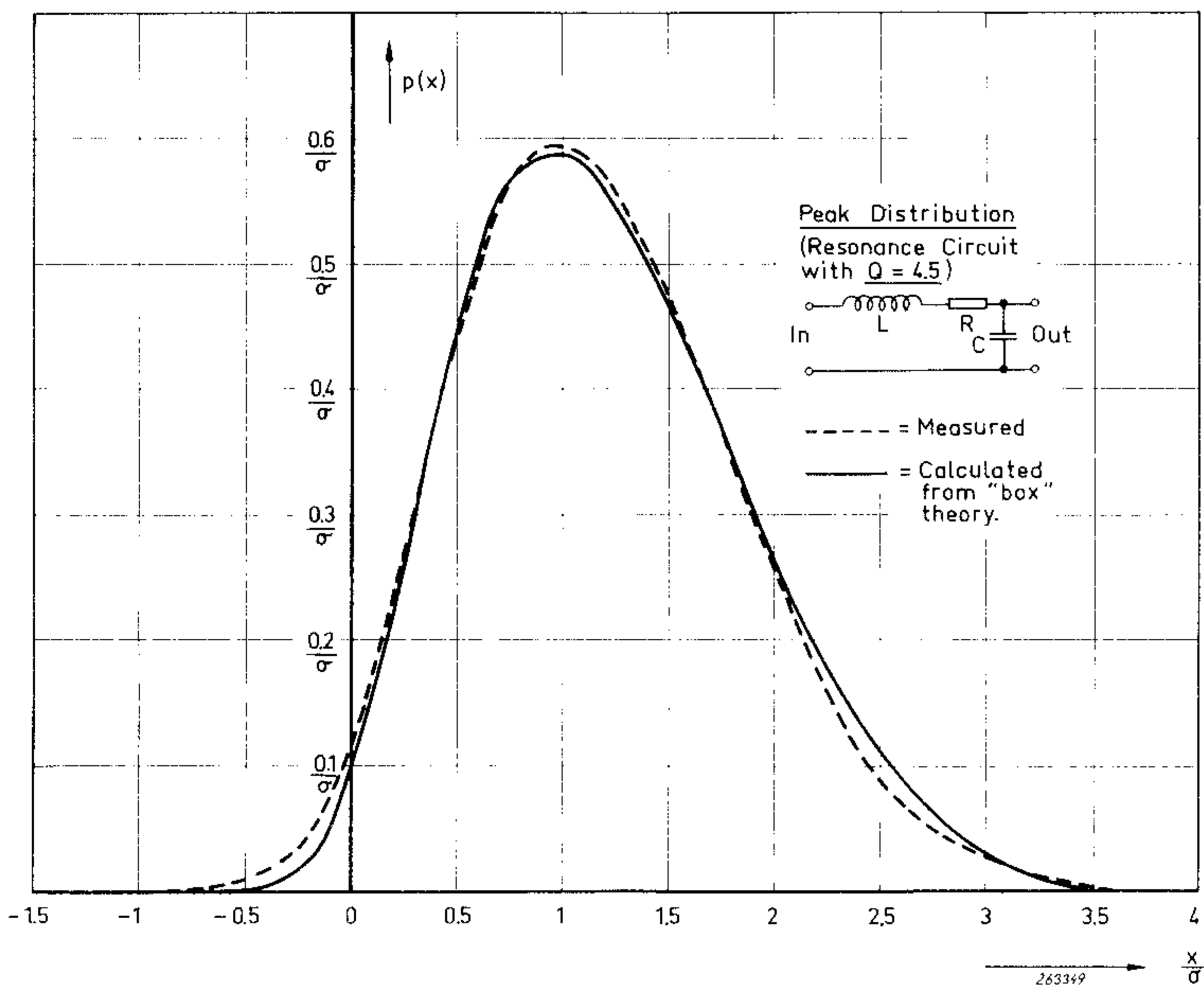
$$\sigma_{\text{box}} = \sqrt{w(f_i) \times Q^2 \times \Delta f_b}$$

Where  $w(f_i)$  and  $Q$  are defined above and  $\Delta f_b$  = width of the "box".

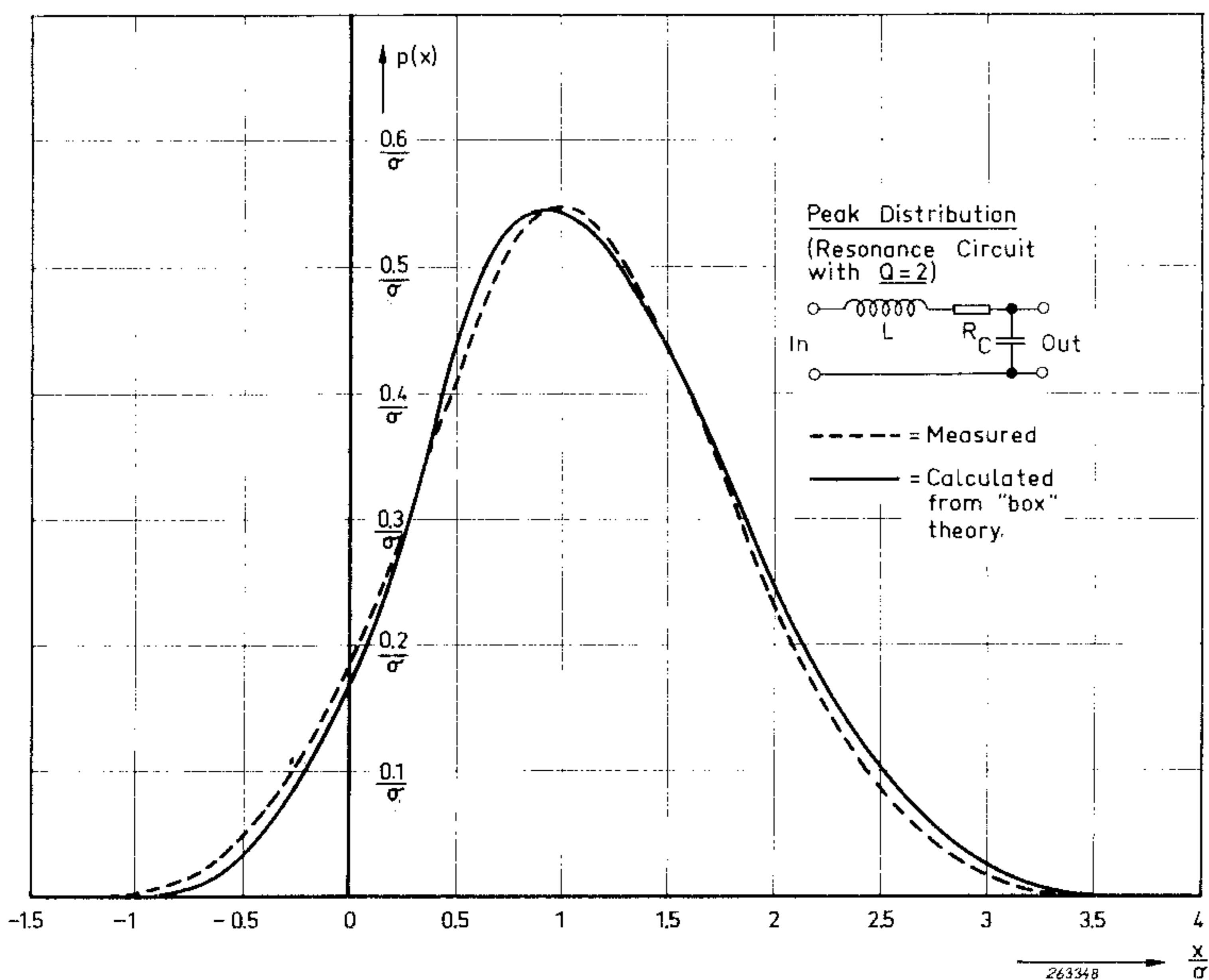
Thus setting  $\sigma_{\text{res}} = \sigma_{\text{box}}$  gives  $\Delta f_b = \frac{\pi}{2} \times \Delta f_r$ .



a)



b)



c)

Fig. 19. Examples of peak probability density curves for single degree of freedom systems with different  $Q$ -values and an "end" slope towards higher frequencies of  $-12$  dB/octave:

- a)  $Q = 9$
- b)  $Q = 4.5$
- c)  $Q = 2$

the forcing spectrum falls off above the resonance frequency) due to the  $-6$  dB/octave end-slope of the spectrum towards higher frequencies.

In the case of Fig. 7 (c) a single “box”-approximation cannot be used at all. However, this type of spectrum is not likely to be met in practice, as normally the forcing spectrum itself drops off towards higher frequencies and the case will not be treated further here. It may, however, be mentioned that very low  $\alpha$ -values can be obtained from this type of spectrum which is also evident from the investigations of the “theoretical spectra” on p. 13.

The “box”-approximation introduced above is very convenient to use for the approximate treatment of the peak distributions, especially in cases where the spectrum contains a number of resonance peaks, such as multi-degree-of-freedom systems. This will be shown in the following.

### **Multi-degree of Freedom Systems.**

A mechanical system in which the masses can move independently or in more than one direction is commonly termed, a multi-degree of freedom system. When the frequency response of such a system is plotted it will normally show one resonance (natural frequency) per independent movement, so that a two degrees of freedom system shows two resonance peaks, a three degrees of freedom system shows three resonance peaks, etc.

A two degrees-of-freedom mechanical system is sketched in “block-diagram form” in Fig. 20 together with its electrical analogue circuit (mobility analogy). This system may for example consist of a mass, say a compact instrument packed for shipping in a case lined with some elastic damping material and the whole package secured to the deck of a ship for transport. Or a simplified “equivalence” of a car moving on the road, the “first” resonance system consisting of the rubber tires and the mass of the wheels and axles, and the second of the mass of the whole car chassis and its suspension. Actually both the above mentioned analogues are “practical” simplifications for more complicated systems but may serve as illustrating examples. The frequency response of the two-degrees-of-freedom system considered in Fig. 20 is shown in Fig. 21 (a). Fig. 21 (b) shows the equivalent “box-filter”-response. As stated in the discussion of the single-degree-of-freedom system a requirement for the “box-filter” approach to the problem to be a good approximation is that the high frequency drop-off of the highest resonance has a fairly steep slope ending in at least  $-12$  dB/octave and that the  $-3$  dB band-width of the resonance is less than about 1/1 octave. These conditions are normally fulfilled in practical vibration problems. The frequency response plotted in Fig. 21 refers to the velocity (displacement) as measured on the “second” mass when the forcing signal consists of a constant velocity (displacement). Other types of measurements, or forcing signals will give different frequency responses. When systems with a frequency response of the type shown are subjected to wide band noise input vibrations, a relatively simple formula for  $\alpha$ , governing the peak distribution of the response, can be worked out on the basis of the “box”-approximation.

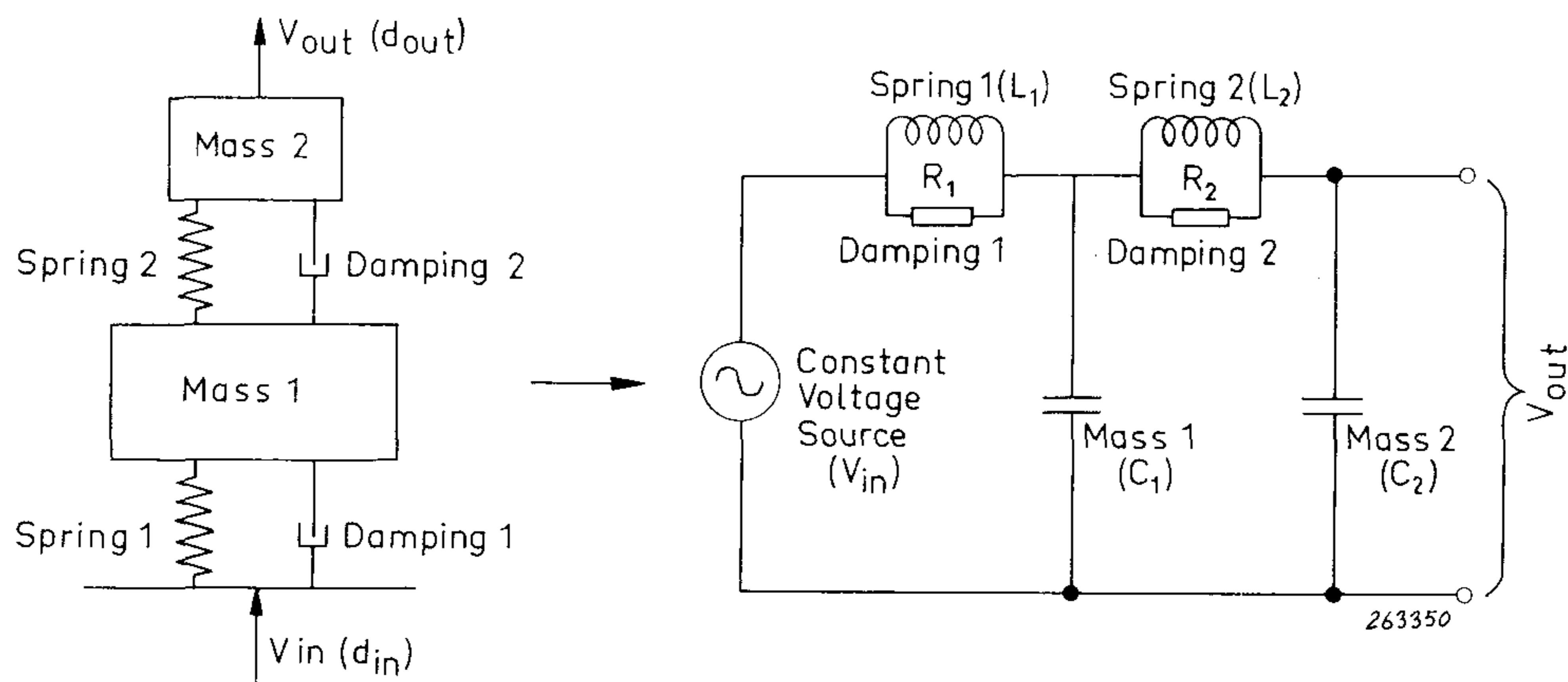


Fig. 20. Example of a two degrees of freedom system and its electrical analogue (mobility analogy).

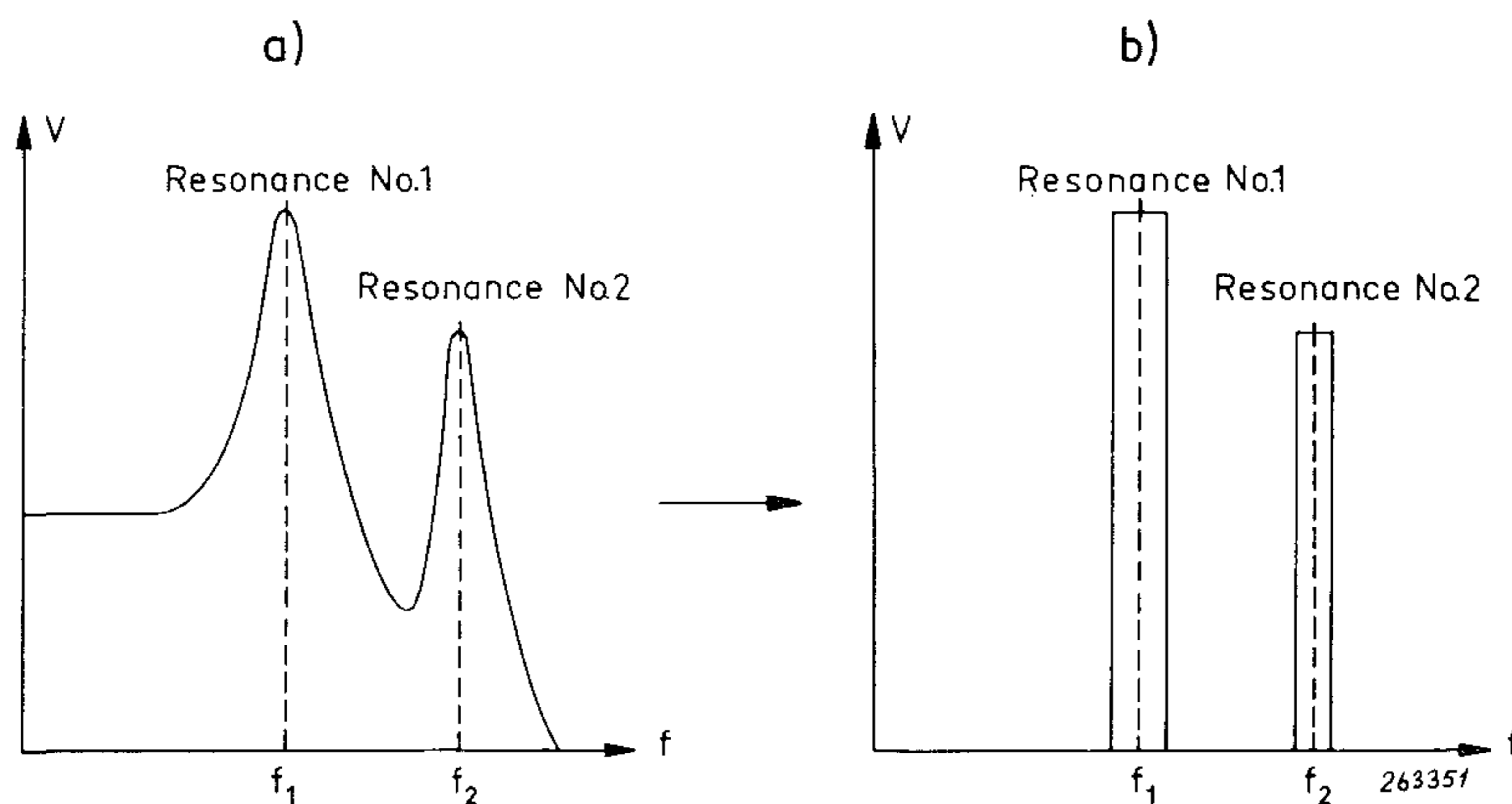


Fig. 21. Typical frequency response curve for a two degrees of freedom system and its "box"-equivalent spectrum.

It is then possible to plot a set of curves of  $\alpha$  vs. the ratio between the two resonance frequencies,  $\frac{f_2}{f_1}$ , with the ratio  $\beta = \frac{\Psi_2}{\Psi_1}$  as parameter ( $\Psi_{01}$  = energy contained in resonance No. 1,  $\Psi_{02}$  = energy contained in resonance No. 2). The curves are shown in Fig. 22 and reveal a number of interesting results.

Firstly it can be seen that when the energy contained in resonance No. 2 is *very* small compared to the energy contained in resonance No. 1 the peak distribution remains a true Rayleigh distribution ( $\alpha = 1$ ) until the ratio between the resonances frequencies,  $\frac{f_2}{f_1}$ , is relatively great. This can be explained when the maximum slopes and amplitudes of the "two" noise signal wave-shapes (two resonances) are considered. (To obtain a small peak-notch combination it is necessary that the slope of the wave-shape of the high frequency signal is greater than the slope of the low frequency signal).



$$\alpha = \frac{[1 + (\frac{f_2}{f_1})^2 \beta]^2}{[1 + \beta][1 + (\frac{f_2}{f_1})^4 \beta]}$$

$$\beta = \frac{C_2 \cdot \Delta f_2}{C_1 \cdot \Delta f_1} = \frac{\psi_{02}}{\psi_{01}} = \left(\frac{\sigma_2}{\sigma_1}\right)^2$$

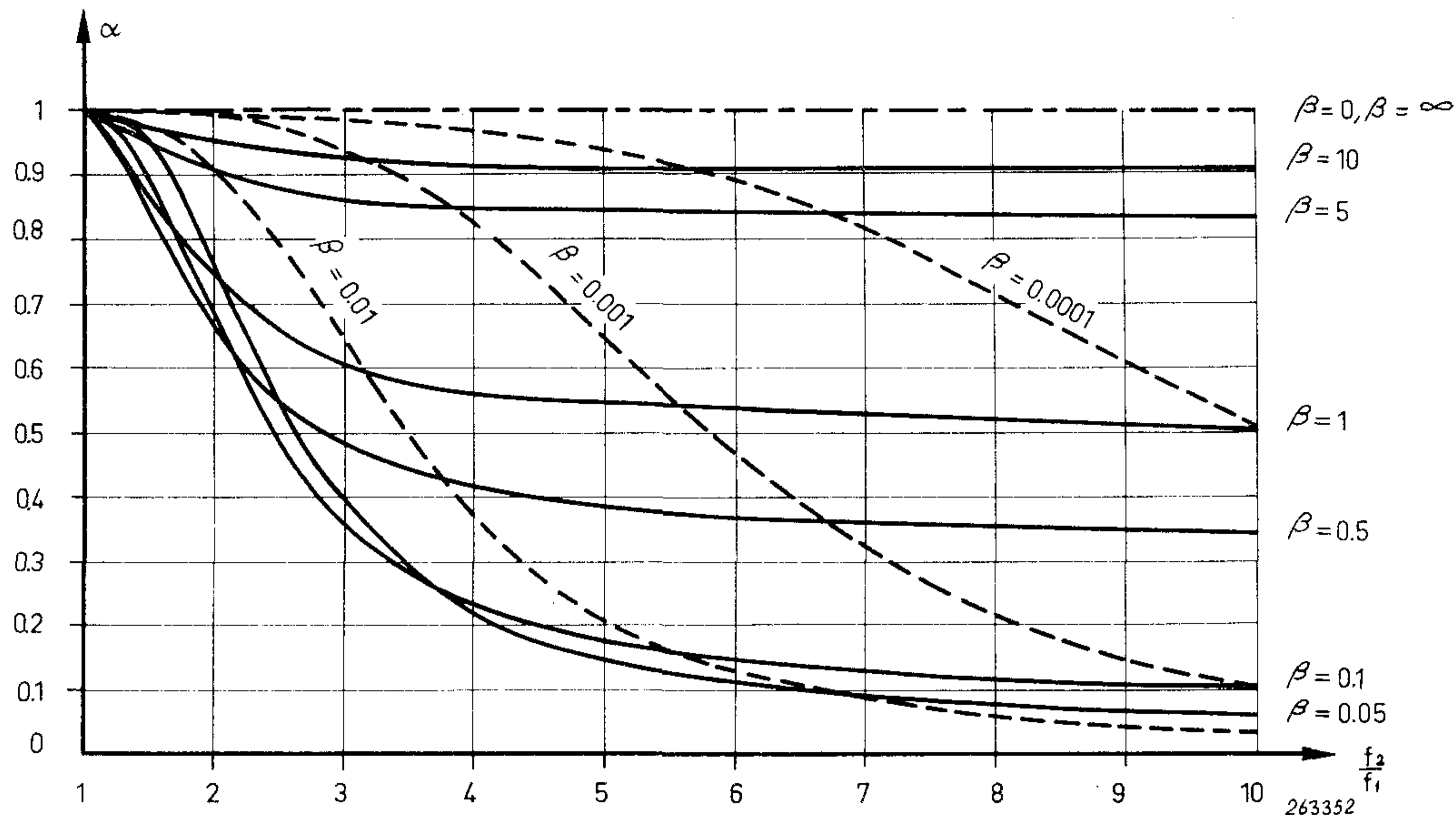


Fig. 22. Curves derived from the "box"-approximation and showing the dependency of  $\alpha$  upon the ratio between the two resonance frequencies of a two degrees of freedom system. The energy-ratio,  $\beta$ , is used as parameter. Dotted curves refer to very small energy ratios and will most probably be of little practical interest.

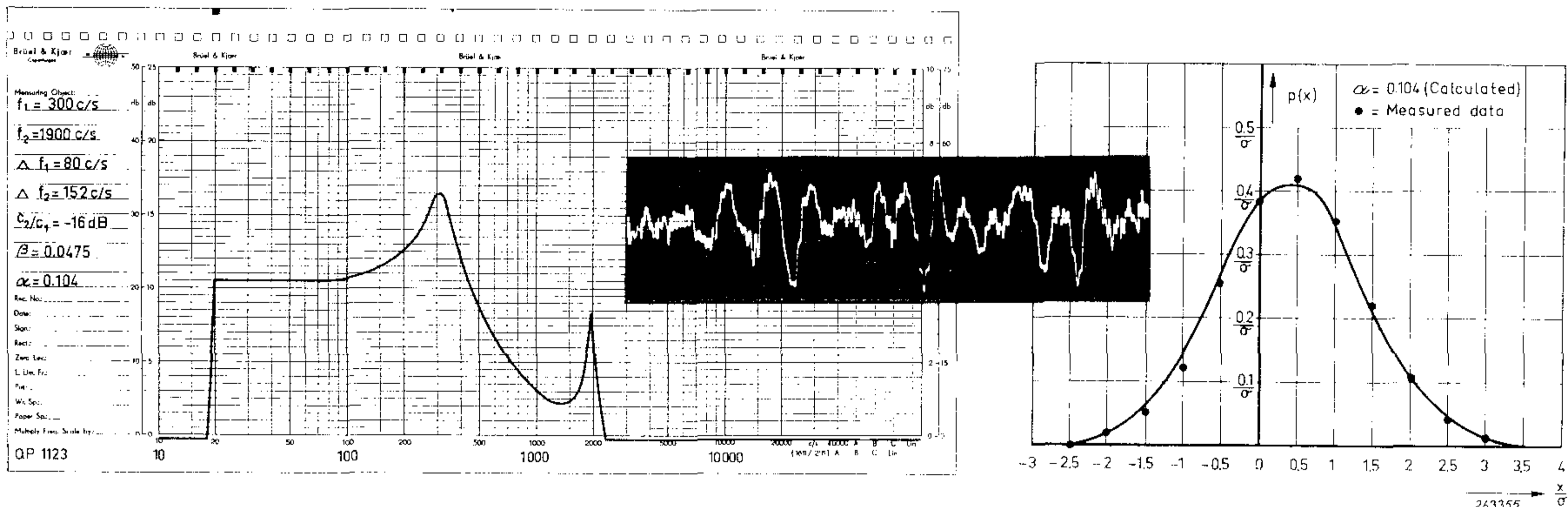
Secondly, the same  $\alpha$ -value can be obtained for a fixed  $\frac{f_2}{f_1}$ -ratio with different  $\beta$ -values, namely in one case when  $\beta$  is *very* small and in the second when  $\beta$  is considerably greater. In the case when  $\beta$  is very small the peaks and notches caused by the high frequency signal (resonance No. 2) are so small that they will be of little, if any, importance in vibration problems, and only the second case, when  $\beta$  is considerably higher, need to be considered seriously.

The validity of the curves given in Fig. 22 has been checked experimentally on analogue models as outlined above. Some of the results are given in Figs. 23 and 24 and by comparing the  $\frac{f_2}{f_1}$ ,  $\beta$ , and  $\alpha$ -values obtained from the measurements with those given by the curves in Fig. 22 it is seen that a very good correlation exists between the theoretical and practical results. Samples of the signal wave-shapes are also shown and demonstrate very nicely the linear superposition of the high and low frequency resonance bands.

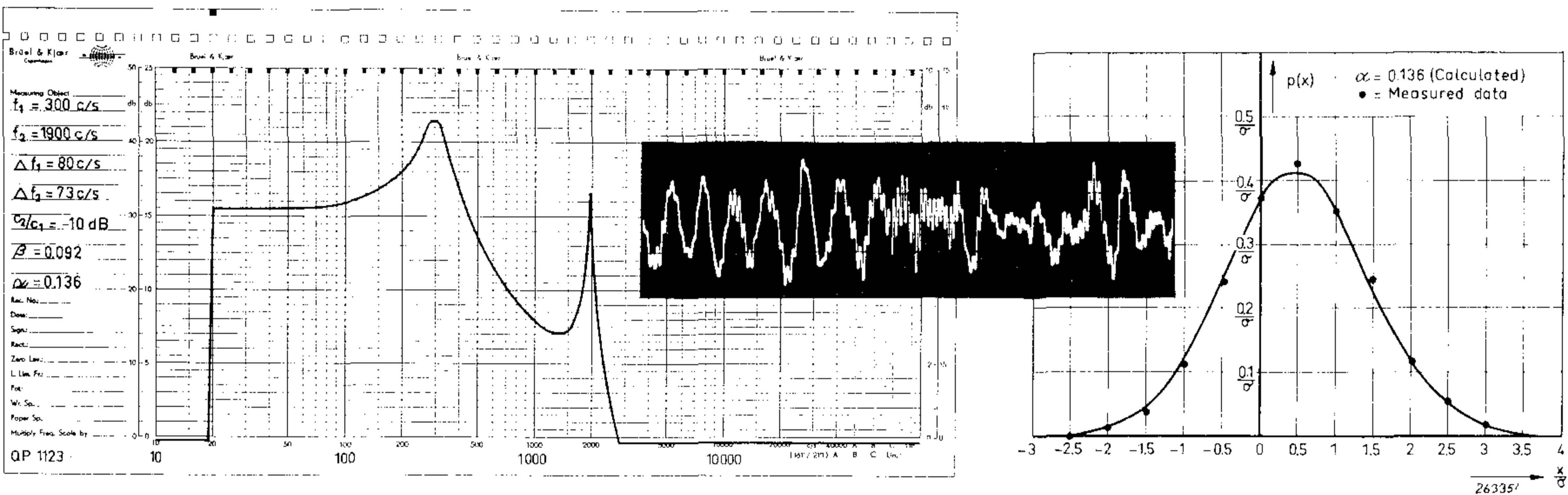
Finally it may be mentioned that the formula found for  $\alpha$  in the case of a two-degrees-of-freedom system, and given in Fig. 22, can easily be extended to multi-degrees-of-freedom systems. It will then take the form:

$$\alpha = \frac{[1 + \sum_n \left(\frac{f_n}{f_1}\right)^2 \times \beta_n]^2}{[1 + \sum_n \beta_n] \times [1 + \sum_n \left(\frac{f_n}{f_1}\right)^4 \times \beta_n]}$$

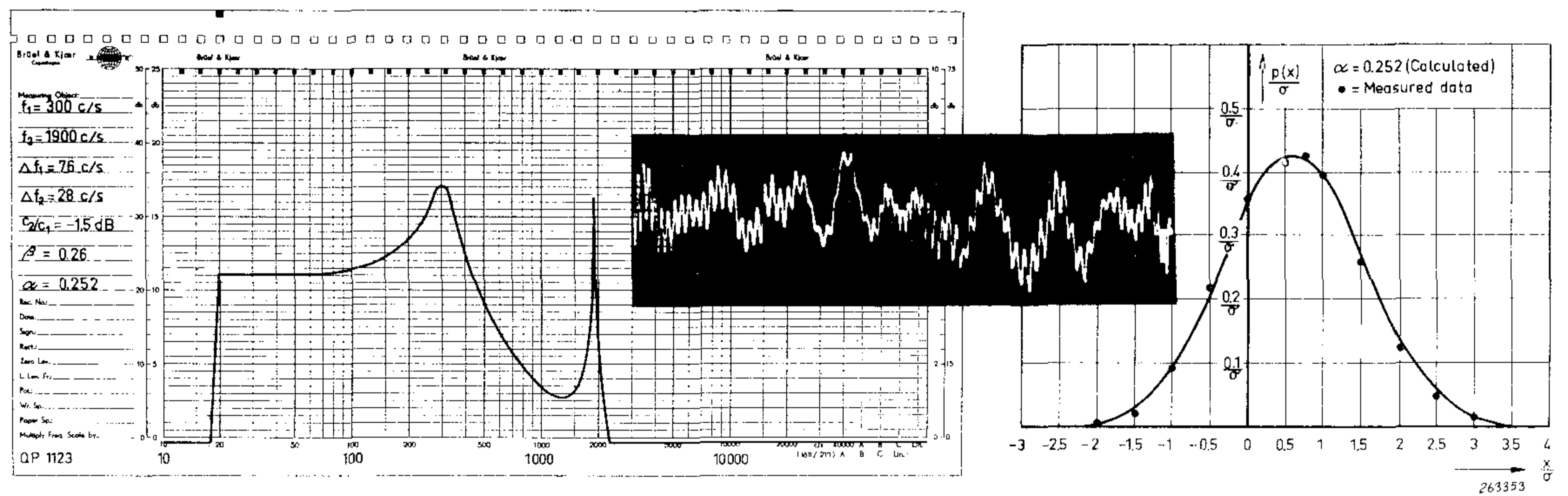
where  $f_n$  is the center frequency of the  $n$ 'th resonance and  $\beta_n = \frac{c_n}{c_1} \times \frac{\Delta f_n}{\Delta f_1}$ . It



a)



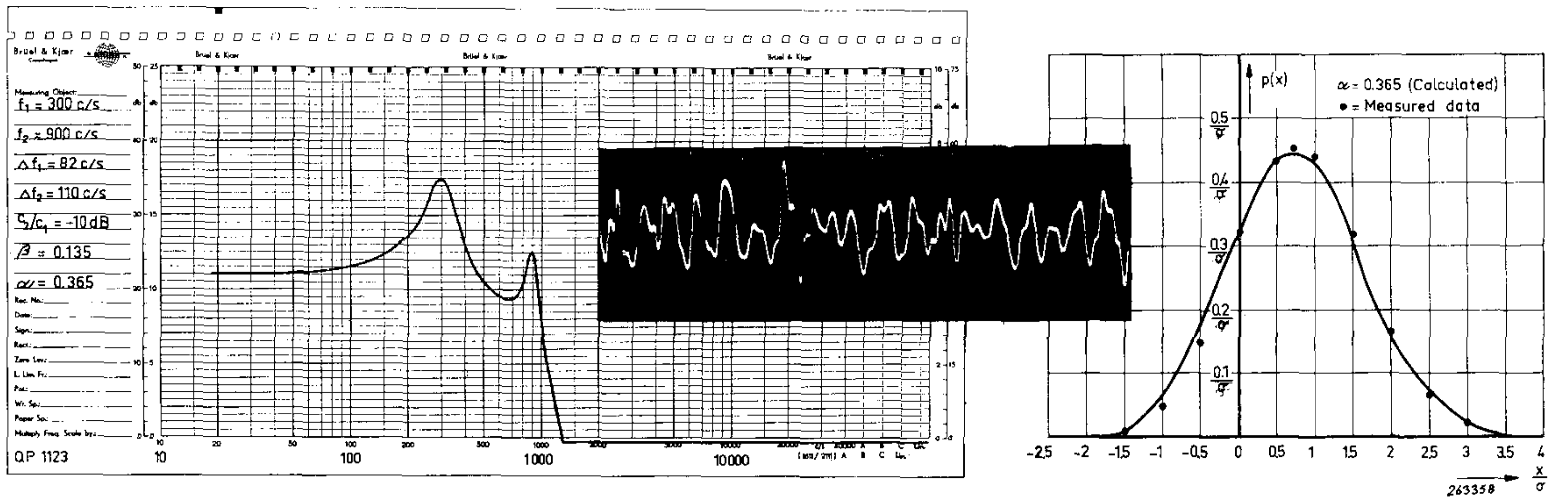
b)



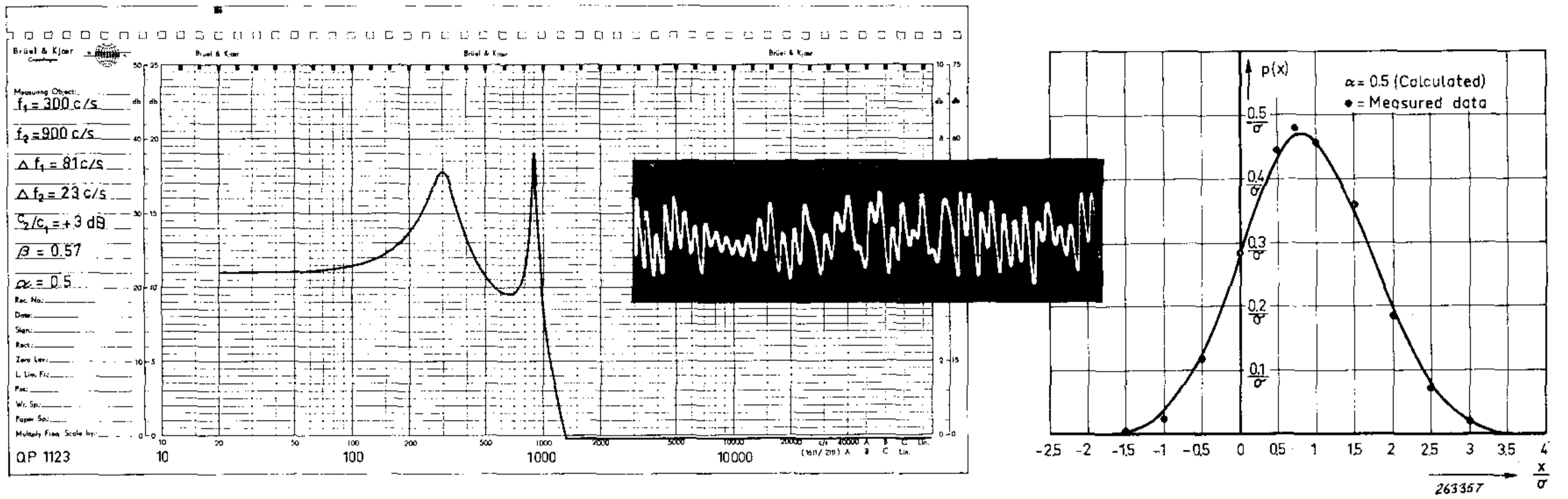
c)

Fig. 23. Experimental results obtained from measurements on a two degrees of freedom system. Both frequency response curves, peak probability density curves and samples of the signal wave shape are shown. The two resonance frequencies were 300 c/s and 1900 c/s respectively.

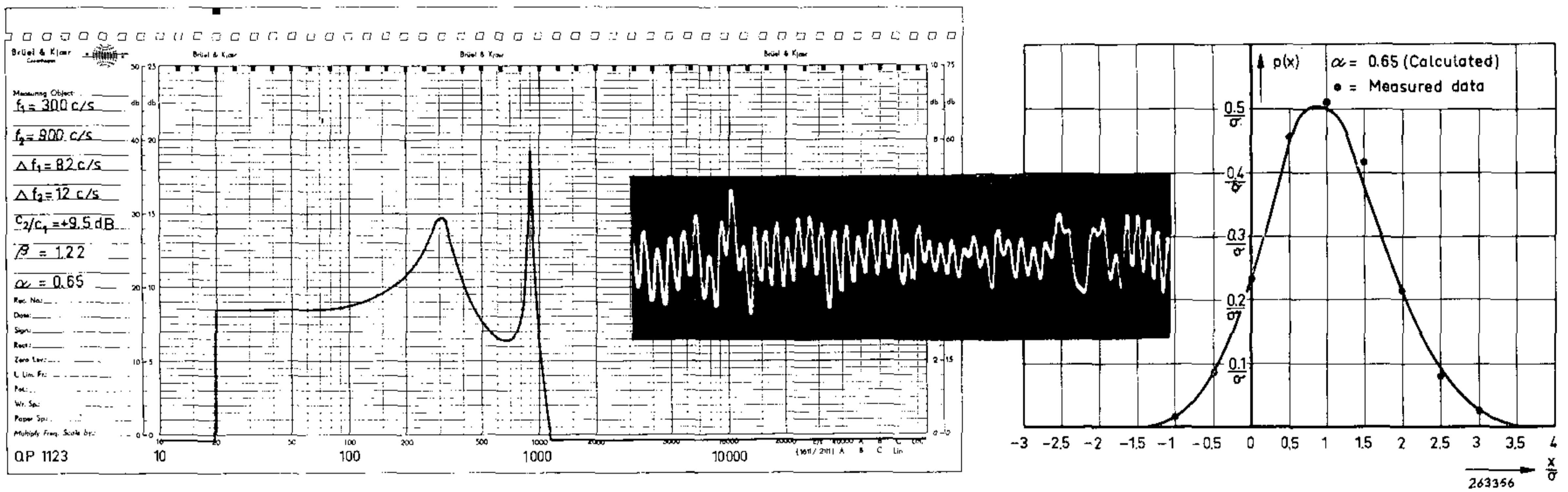
- a)  $\beta = 0.0475$  ( $\alpha = 0.104$ )
- b)  $\beta = 0.092$  ( $\alpha = 0.136$ )
- c)  $\beta = 0.26$  ( $\alpha = 0.252$ )



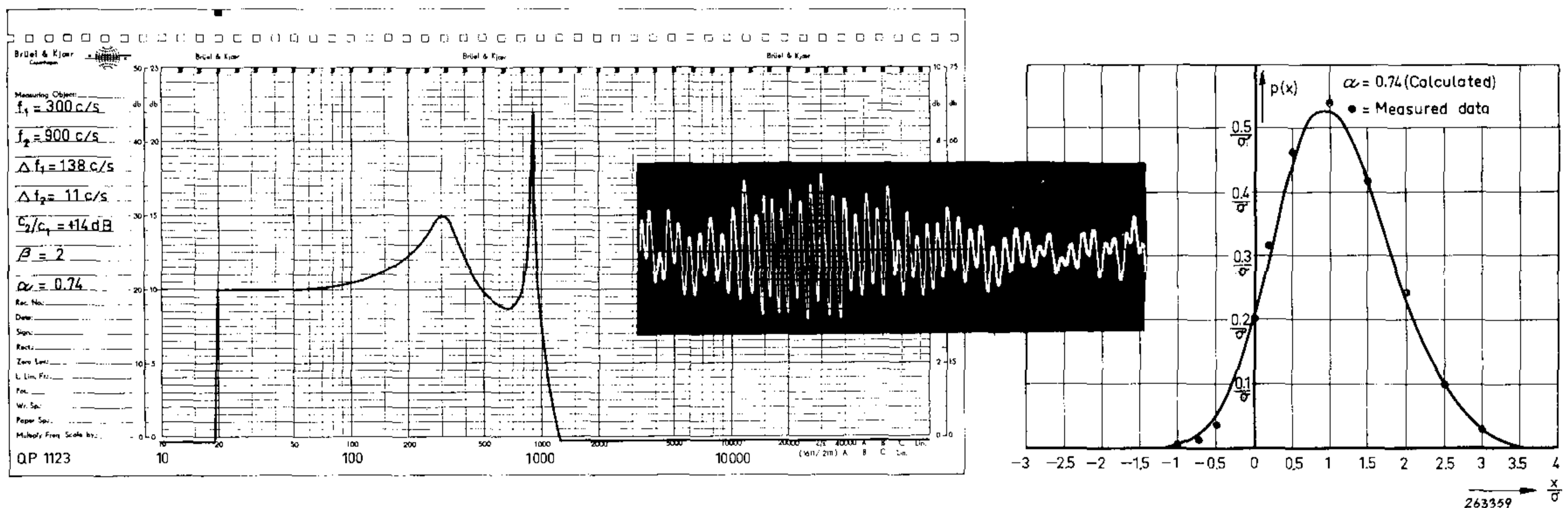
a)



b)



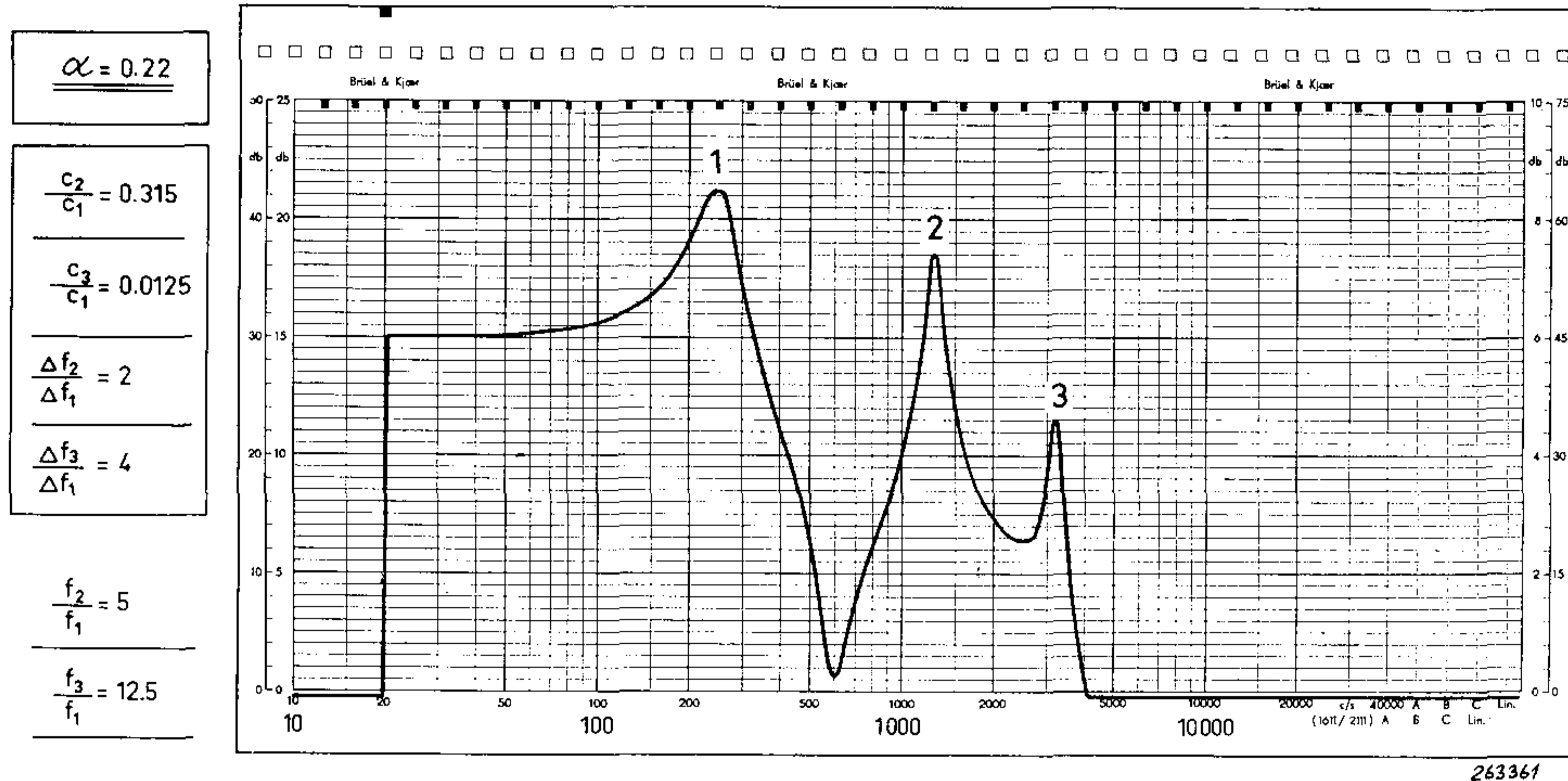
c)



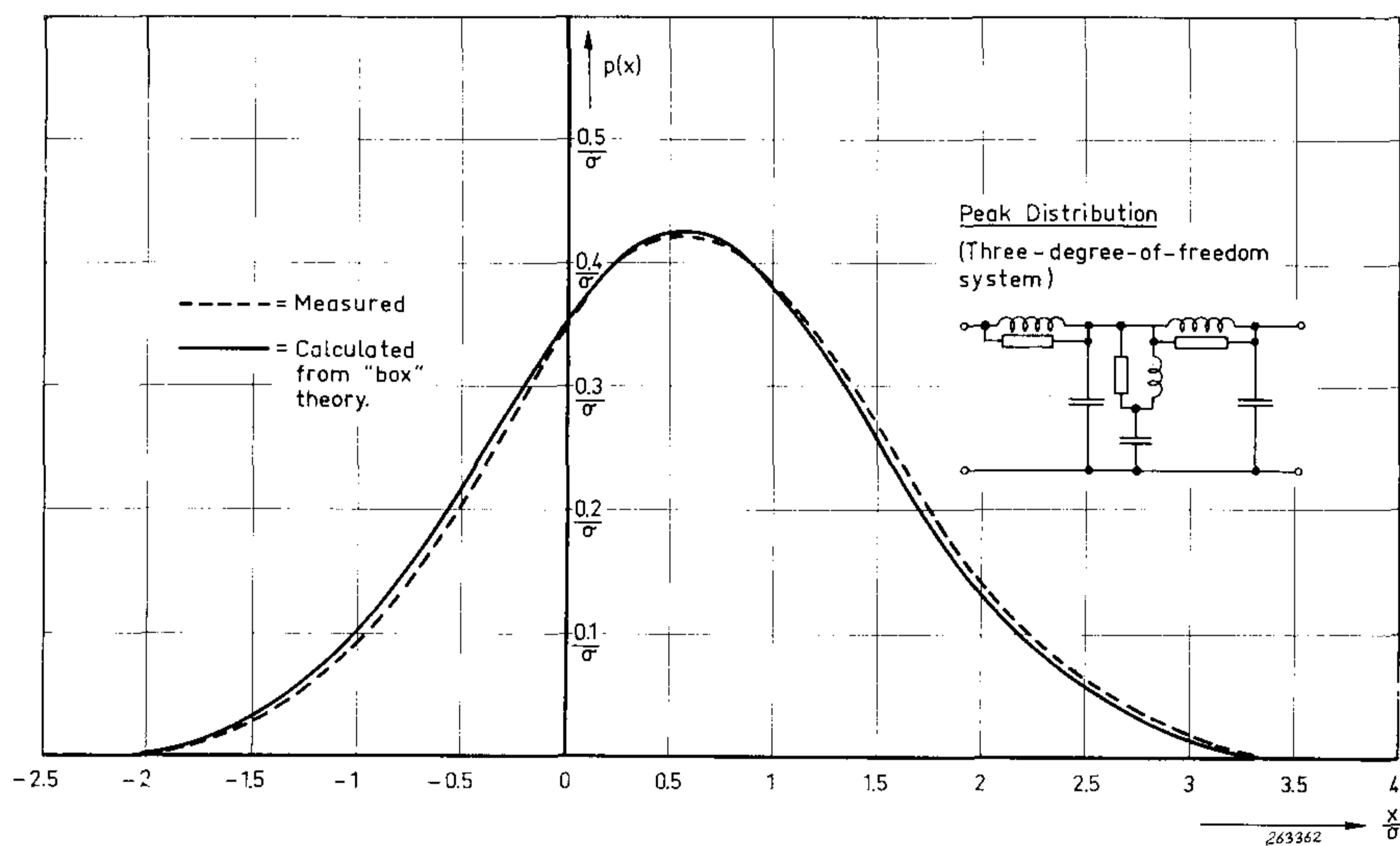
d)

Fig. 24. Similar to Fig. 23. However, the two resonance frequencies were in this case 300 c/s and 900 c/s.

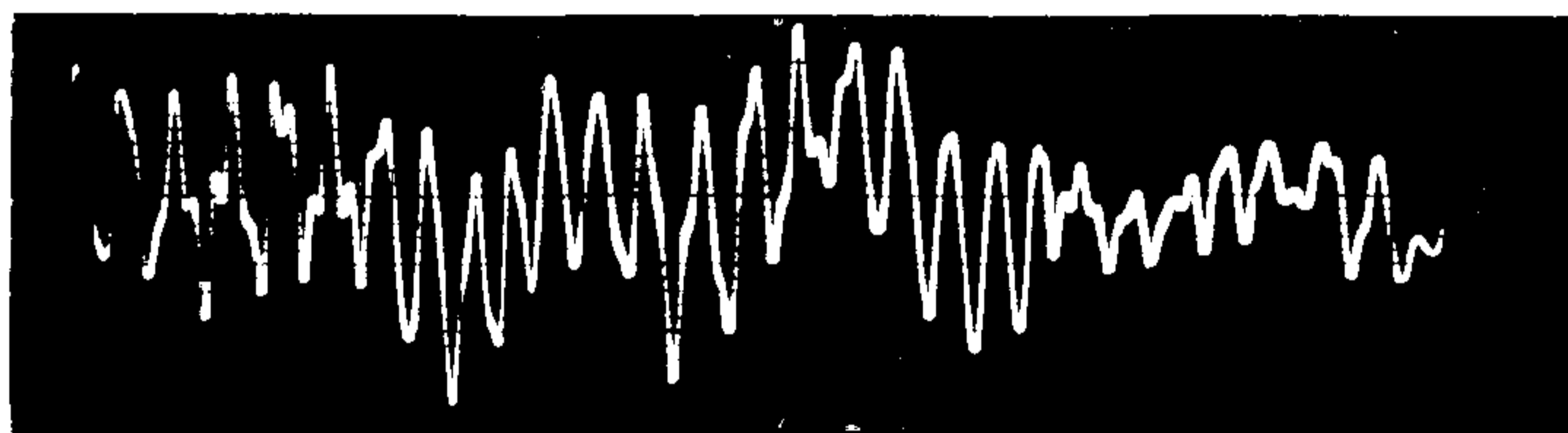
a)  $\beta = 0.135$  ( $\alpha = 0.365$ )      c)  $\beta = 1.22$  ( $\alpha = 0.65$ )  
 b)  $\beta = 0.57$  ( $\alpha = 0.5$ )      d)  $\beta = 2$  ( $\alpha = 0.74$ )



a)



b)



c)

Fig. 25. Frequency response, peak probability density curve, analogue circuit and samples of the wave shape for a three degrees of freedom system excited by wide band "white" noise.

- a) Frequency response.
- b) Peak probability density curve and analogue circuit.
- c) Sample of the output wave-shape.

should be pointed out here that  $\frac{c_n}{c_1}$  is the **energy**-ratio between the responses of the two resonance peaks corresponding to the frequency  $f_n$  and  $f_1$ . Thus, if this ratio is read from a chart recording calibrated in dB, a difference of

— 10 dB between the resonance peaks corresponds to  $\frac{c_n}{c_1} = 0.1$ .

The bandwidths  $\Delta f_n$  and  $\Delta f_1$  are read directly off the chart at the — 3 dB points.

As an example of the use of the formula given above, a three-degrees-of-freedom system having the frequency response shown in Fig. 25 (a), was investigated. The values of  $\frac{c_n}{c_1}$ ,  $\Delta f_n$  and  $f_n$  were determined from the response measurements as indicated in the figure, and the resulting  $\alpha$ -value calculated. By feeding the circuit from the Random Noise Generator and measuring the peak distribution the result shown in Fig. 25 (b) was obtained. Note the good correlation between the calculated and the measured  $\alpha$ -value. Finally Fig. 25 (c) shows a sample of the signal wave-shape.

### **Conclusion.**

A study has been made of the dependency of the distribution of random noise maxima upon the shape of the noise spectrum. It was found that the exact mathematical theory as given by S. O. Rice may be “modified” when applied to practical vibration problems. The main reason for a possible “modification” is that the exact theory does not distinguish between the infinitely small peaks and notches and the more important greater peaks and notches occurring in wide band noise signals. Peak distributions obtained from the exact mathematical theory deviate, in some cases from those measured in practice, where the very small peaks and notches are not accounted for. It is suggested that a “box”-approximation may be used for the treatment of resonant systems with amplification factors (Q-values) greater than around 2 and a steepness of the end-slope towards higher frequencies of at least — 12 dB/octave.

The “box”approximation also simplifies the treatment of more complicated, multi-degrees-of-freedom systems as commonly met in vibration practice considerably. Good agreement has been found between the results obtained from “box”-approximations, and practical measurements.

### **Acknowledgement.**

The author wishes at this point to thank Mr. Carl G. Wahrmann of Brüel & Kjær for many valuable discussions during the preparation of this paper, and for redesigning the circuitry of the electronic counter used in the experimental part of the work.

**Selected References:**

- J. S. BENDAT: "Principles and Applications of Random Noise Theory", John Wiley & Sons Inc. 1958.
- J. S. BENDAT et. al.: "The Application of Statistics to the Flight Vehicle Vibration Problem", ASD Technical Report 61-123, U.S. Department of Commerce, Office of Technical Services.
- L. L. BERANEK: "Acoustics", Mc.Graw-Hill Book Company Inc. 1954, New York, Toronto, London.
- S. H. CRANDALL et. al.: "Random Vibration", John Wiley & Sons, Inc., New York, M.I.T. 1958.
- C. M. HARRIS and C. E. CREDE: "Shock and Vibration Handbook", Mc.Graw-Hill Book Company, 1961, New York, Toronto, London.
- J. P. den HARTOG: "Mechanical Vibrations", Mc.Graw-Hill Book Company, Inc. 1956, New York, Toronto, London.
- J. R. PIERCE: "Physical Sources of Noise", Proc. of the I. R. E., Vol. 44, May 1956, U.S.A.
- S. O. RICE: "Mathematical Analysis of Random Noise", Bell System Techn. Journal 23 (1944) and 24 (1945).  
Also contained in N. Wax: "Selected Papers on Noise and Stochastic Processes", Dover Publications Inc. New York 1954.

## Appendix

### Brief Theory of the Distribution of Maxima

The formula given on page 8 has been derived from the original work of S. O. Rice of the Bell Telephone Laboratories Inc. on mathematical analysis of random noise. His general equation for the distribution of noise maxima in amplitude-linear systems was obtained by studying the combined properties of  $x$ ,  $\frac{dx}{dt}$  and  $\frac{d^2x}{dt^2}$  of the noise, assuming that  $x(t)$  is a normal Gaussian process in time. A maximum (peak) is then obtained when  $\frac{dx}{dt} = 0$  and  $\frac{d^2x}{dt^2}$  is negative. Using his notation the expectance of a maximum occurring in the rectangle  $dx \times dt$  is:

$$P(x, x + dx; t, t + dt) = \frac{dx dt}{M_{33}} \frac{1}{\sqrt{8 \pi^3}} \left[ |M|^{1/2} \exp\left(-\frac{M_{11} x^2}{2 |M|}\right) + M_{13} x \left(\frac{\pi}{2 M_{33}}\right)^{1/2} \left(1 + \operatorname{erf} \frac{M_{13} x}{(2 |M| M_{33})^{1/2}}\right) \exp\left(-\frac{x^2}{2 \psi_0}\right) \right] \quad (\text{A1})$$

where

$$\begin{aligned} |M| &= -\Psi_0'' (\Psi_0 \Psi_0^{(4)} - \Psi_0''^2) \\ M_{11} &= -\Psi_0'' \Psi_0^{(4)} \\ M_{13} &= \Psi_0''^2 \\ M_{33} &= -\Psi_0'' \Psi_0 \end{aligned}$$

and

$$\begin{aligned} \Psi_0 &= \int_0^\infty \omega(f) df \\ \Psi_0'' &= -4 \pi^2 \int_0^\infty f^2 \omega(f) df \\ \Psi_0^{(4)} &= 16 \pi^4 \int_0^\infty f^4 \omega(f) df \end{aligned}$$

Here  $\omega(f)$  is the input power spectral density.

To obtain an expression for the **probability density** of the maxima (A1) has to be divided by the total number of maxima  $P_{\text{Max. tot.}}$  occurring in the time interval  $t$  to  $t + dt$ . Here again one of Rice's results is used:

$$P_{\text{Max. tot.}} = \frac{dt}{2 \pi} \left[ \frac{\Psi_0^{(4)}}{-\Psi_0''} \right]^{1/2}$$

The probability density function for the maxima then becomes:

$$p(x) dx = \frac{P(x, x + dx; t, t + dt)}{P_{\text{Max. tot.}}} \quad (\text{A2})$$

Inserting the values for  $|M|$ ,  $M_{11}$ ,  $M_{13}$ ,  $M_{33}$  and  $P_{\text{Max. tot}}$  into equation (A2) gives:

$$\frac{1}{\sqrt{8 \pi^3}} \frac{|M|^{1/2}}{M_{33}} = \frac{1}{\sqrt{2 \pi}} \sqrt{\frac{1}{\Psi_0} \left( 1 - \frac{\Psi_0''^2}{\Psi_0 \Psi_0^{(4)}} \right)} = \underline{\underline{\frac{1}{\sigma \sqrt{2 \pi}} \sqrt{1 - \alpha}}}$$

and

$$\frac{M_{11}}{2 |M|} = \frac{1}{2} \frac{-\Psi_0'' \Psi_0^{(4)}}{-\Psi_0'' (\Psi_0 \Psi_0^{(4)} - \Psi_0''^2)} = \frac{1}{2} \frac{1}{\Psi_0 \left( 1 - \frac{\Psi_0''^2}{\Psi_0 \Psi_0^{(4)}} \right)} = \underline{\underline{\frac{1}{2 \sigma^2 (1 - \alpha)}}}$$

and

$$\frac{M_{13} \left( \frac{1}{M_{33}} \right)^{1/2}}{P_{\text{Max. tot.}} 4 \pi} = \frac{1}{2} \frac{\Psi_0''^2}{-\Psi_0'' \Psi_0} \left[ \frac{1}{-\Psi_0'' \Psi_0} \frac{-\Psi_0''}{\Psi_0^{(4)}} \right] = \underline{\underline{\frac{\sqrt{\alpha}}{2 \sigma^2}}}$$

and

$$\frac{M_{13}}{[2 |M| M_{33}]^{1/2}} = \frac{\Psi_0''^2}{[2 \Psi_0''^2 \Psi_0 (\Psi_0 \Psi_0^{(4)} - \Psi_0''^2)]^{1/2}} = \underline{\underline{\frac{1}{\sigma} \sqrt{\frac{\alpha}{2 (1 - \alpha)}}}}$$

where  $\sigma = \sqrt{\Psi_0}$  and  $\alpha = \frac{\Psi_0''^2}{\Psi_0 \times \Psi_0^{(4)}}$

The expression (A2) for the probability density function then becomes:

$$p(x) = \frac{\sqrt{1 - \alpha}}{\sigma \sqrt{2 \pi}} \cdot \exp \left[ -\frac{x^2}{2 \sigma^2 (1 - \alpha)} \right] + \frac{\sqrt{\alpha}}{2 \sigma} \cdot \frac{x}{\sigma} \cdot \left[ 1 + \operatorname{erf} \left( \frac{x}{\sigma} \sqrt{\frac{\alpha}{2 (1 - \alpha)}} \right) \right] \exp \left[ -\frac{x^2}{2 \sigma^2} \right]$$

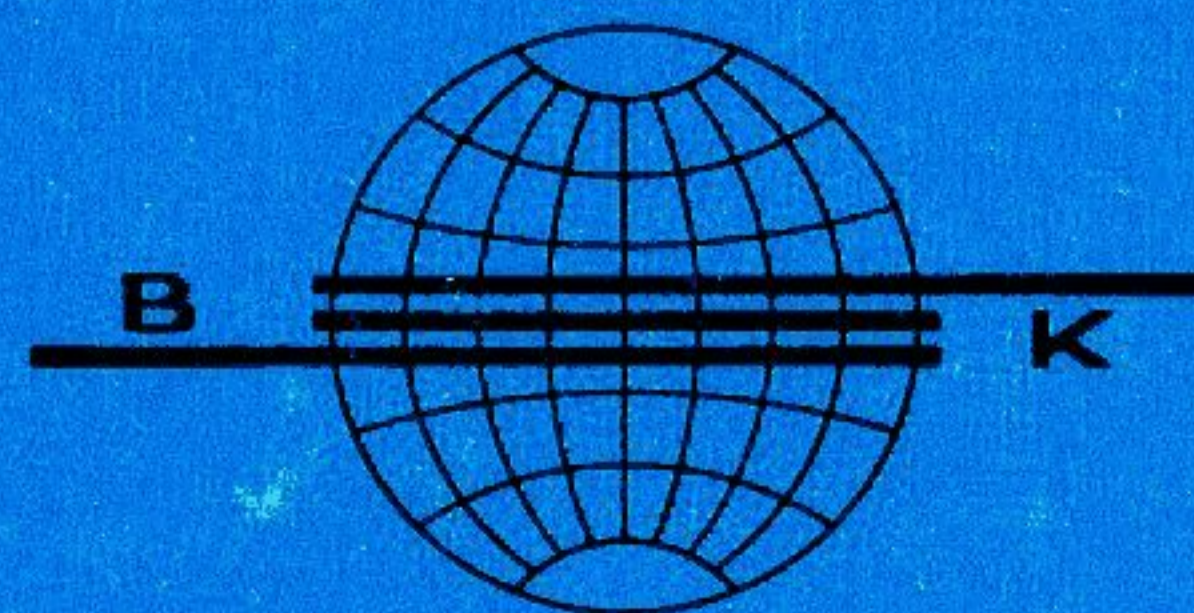
which is the expression given on page 8.

It is interesting to note the "meaning" of the quantity here called  $\alpha$ . Again using some of Rice's results  $\alpha$  is equal to  $\left( \frac{z}{2m} \right)^2$  where  $z$  is the total number of zero crossings and  $m$  is the total number of noise maxima per second. The Rayleigh distribution is obtained for  $\alpha = 1$ , i.e. when there is exactly two zero crossing per peak! (Modulated sine wave). A Gaussian distribution is obtained when  $\alpha = 0$ , i.e. when there is infinitely many peaks per zero crossing.



# Brüel & Kjær

ADR.: BRÜEL & KJÆR  
NÆRUM - DENMARK



TELEX 5316

TELEPHONE: 800500  
⚡ BRUKJA, Copenhagen